The Pennsylvania State University
APPLIED RESEARCH LABORATORY
P.O. Box 30
State College, PA 16804

THE EVALUATION OF A PROPELLER UNSTEADY FORCE COMPUTER PROGRAM TO PREDICT PROPELLER INDUCED UNSTEADY HULL PRESSURES

by

W. G. Berberich
R. C. Marboe

Technical Report No. TR 91-009
July 1991

A-1

Supported by:
Naval Sea Systems Command

L.R. Hettche, Director
Applied Research Laboratory

Approved for public release; distribution unlimited

REPORT DOCUMENTATION PAGE

Form Approved
OMB No. 0704-0188

1. AGENCY USE ONLY (Leave blank)	2. REPORT DATE	3. REPORT TYPE AND DATES COVERED
	May 1991	

4. TITLE AND SUBTITLE
The Evaluation of a Propeller Unsteady Force Computer Program to Predict Propeller Induced Unsteady Hull Pressures

5. FUNDING NUMBERS
N-00039-88-C-0051

6. AUTHOR(S)
William G. Berberich

7. PERFORMING ORGANIZATION NAME(S) AND ADDRESS(ES)
Applied Research Laboratory
The Pennsylvania State University
P. O. Box 30
State College, PA 16802

8. PERFORMING ORGANIZATION REPORT NUMBER
TR-91-009

9. SPONSORING/MONITORING AGENCY NAME(S) AND ADDRESS(ES)
Naval Sea Systems Command
Department of the Navy
Washington, DC 20362

10. SPONSORING/MONITORING AGENCY REPORT NUMBER

11. SUPPLEMENTARY NOTES

12a. DISTRIBUTION/AVAILABILITY STATEMENT

12b. DISTRIBUTION CODE

13. ABSTRACT *(Maximum 200 words)*

A potential flow computer program is used to predict the unsteady pressure field on a hullform caused by a rotating propeller. It was chosen over two other approaches and three programs. The program, PUF-3A, uses lifting surface theory and contains variables that are run in different combinations to ascertain their effects. The results are plots of sound pressure level, SPL, versus distance across the hullform and are compared to water tunnel model data.

The baseline experimental configuration is a model of a single screw five blade propeller powered in the wake of a broad, relatively flat hull in a 48-inch water tunnel. Another configuration tests an inflow altering device with the same hull and propeller geometry.

The desired result is an identification of the program's strengths and weaknesses versus water tunnel data. Its strengths were in predicting the relative SPLs of the first blade rate harmonics in two different wake fields. In the case of a simple wake field, the overall relative SPLs of the second and third harmonics compare reasonably well with water tunnel data.

14. SUBJECT TERMS
Potential Flow
Unsteady Pressure Field
hullform
rotating propellor
lifting surface
sound pressure level
rate harmonics

15. NUMBER OF PAGES
57

16. PRICE CODE

17. SECURITY CLASSIFICATION OF REPORT	18. SECURITY CLASSIFICATION OF THIS PAGE	19. SECURITY CLASSIFICATION OF ABSTRACT	20. LIMITATION OF ABSTRACT
UNCLASSIFIED	UNCLASSIFIED	UNCLASSIFIED	UNLIMITED

ABSTRACT (Continued)

The program's main weaknesses are based on its potential flow appraoch with its hydrodynamic assumptions of blade similarity, thin boundary layers, and lack of viscosity and vorticity. The water tunnel data taken with the modified wake presents a more complicated flow towards the center of the propeller. For this case, the program does not predict the overall increase in SPL for the second and third harmonics. The program's limitations increase with the complexity of the flow field. The complexities in this case are shed vorticies from the appendages interacting with the hull wake all being influenced by the effects of the propeller.

These real factors must be modeled before accurate higher harmonic solutions can be obtained for complex wake flows. This is a useful tool for a first cut prediction of blade rate hull unsteady pressures for most wake fields. For a simple wake field, the overall sound pressure levels for the second and third harmonics, relative to blade rate, can be reasonably predicted.

ABSTRACT

A potential flow computer program is used to predict the unsteady pressure field on a hullform caused by a rotating propeller. It was chosen over two other approaches and three programs. The program, PUF-3A, uses lifting surface theory and contains variables that are run in different combinations to ascertain their effects. The results are plots of sound pressure level, SPL, versus distance across the hullform and are compared to water tunnel model data.

The baseline experimental configuration is a model of a single screw five blade propeller powered in the wake of a broad, relatively flat hull in a 48-inch water tunnel. Another configuration tests an inflow altering device with the same hull and propeller geometry.

The desired result is an identification of the program's strengths and weaknesses versus water tunnel data. Its strengths were in predicting the relative SPLs of the first blade rate harmonics in two different wake fields. In the case of a simple wake field, the overall relative SPLs of the second and third harmonics compare reasonably well with water tunnel data.

The program's main weaknesses are based on its potential flow approach with its hydrodynamic assumptions of blade similarity, thin boundary layers, and lack of

viscosity and vorticity. The water tunnel data taken with the modified wake presents a more complicated flow towards the center of the propeller. For this case, the program does not predict the overall increase in SPL for the second and third harmonics. The program's limitations increase with the complexity of the flow field. The complexities in this case are shed vorticies from the appendages interacting with the hull wake all being influenced by the effects of the propeller.

These real factors must be modeled before accurate higher harmonic solutions can be obtained for complex wake flows. This is a useful tool for a first cut prediction of blade rate hull unsteady pressures for most wake fields. For a simple wake field, the overall sound pressure levels for the second and third harmonics, relative to blade rate, can be reasonably predicted.

TABLE OF CONTENTS

TABLE OF CONTENTS

LIST OF FIGURES

LIST OF TABLES

NOMENCLATURE

Symbol	Description
D	Propeller Diameter
Fn	Froude Number
g_c	Gravitational Constant
J_s	Advance Coefficient based on Ship Speed
n	Revolutions per Second
P	Pressure
P_v	Vapor Pressure
Φ	Velocity Potential Function
r	Propeller Radius Ratio (Relative to Tip Radius)
R	Propeller Blade Tip Radius
ρ	Water Density
σ_s	Cavitation Index
V_s	Ship Speed
X,Y,Z	Orthogonal Coordinates

Subscripts for Orthogonal Coordinates

f	Field Point
n	Unit Vector
s	Source Point

1. INTRODUCTION

The rotation of a ship's propeller causes unsteady forces to be transmitted to the ship's hull. These forces travel to the hull by two main paths; through the propeller shaft to the thrust bearing and through the water. This paper will examine forces transmitted through the water to the ship's hull immediately above the propeller. These forces cause unwanted noise, which affects habitation, and vibration, which fatigues structures and machinery. In the past, the problem was treated with post-construction modifications. The solutions ranged from stiffening the hull to changing to a propeller with a different number of blades. The costs of these methods drove designers and builders to seek analytical tools to predict the problems in the design phase so that solutions could be incorporated into new construction.

There have been many approaches to modeling this problem. An early theory for the excitation due to a non-cavitating propeller was derived by Breslin [1]. In this theory, the loading of the propeller is represented by a system of line vortices. The thickness or displacement of the blades is accounted for by a source-sink distribution. The hull was idealized as an infinite flat plate above the propeller. Breslin [2] later developed the solution with an infinitely long circular cylinder. This more closely

approximated the afterbody of a ship. This potential flow solution is known as the lifting-line method. It is restricted because of its non-viscous nature and its lack of detail in describing areas such as the blade's leading edge, propeller hub, and wake.

Vorus [3] continued the analysis to a ship's hullform by calculating excitation forces. He used a diffraction solution that replaced the flat plate with a source distribution that represents the hull. This diffracted the pressure field and led to a better approximation of the pressures but was very complicated and time consuming. Huse [4] later removed the hull entirely and calculated a free space pressure. He then multiplied these pressures by a "Solid Body" factor, SBF, found experimentally to account for the effects of the hull. Model data were divided by calculations of the free field pressure and the SBF for different types of hulls consistently varied from 1 to 3. Jacobs, Mercier, and Tsakonas [5] did experiments on a model destroyer hull and found agreement with calculations near the propeller with an SBF of 2.

Holden, et. al. [6] were one of the first to use a bottoms-up approach. They gathered full scale data on 72 ships and used a regression analysis with parameters of the problem's geometry and hydrodynamics. The compared data have a 25% standard deviation. This approach was not satisfactory as a prediction scheme because of the large

variation. Other empirical techniques were tried with similar results.

Kerwin and Lee [7] developed a fully three-dimensional unsteady computer program based on lifting surface theory. This method predicts unsteady non-cavitating propeller performance using a discrete singularity method and was later extended by Lee [8] to treat partially cavitating propellers. This work has been updated in its treatment of the cavitation problem [9]. The result is the computer program Propeller Unsteady Force (PUF-3A) [10]. The program is accompanied by a host of subprograms that incorporate routines for calculation of local blade forces, wake processing, and field point potential.

The current method of analysis uses lifting surface theory. This paper examines four lifting surface codes and two quick look empirical techniques. The Massachusetts Institute of Technology's PUF-3A and family of subprograms appear to promise the most success. The PUF-3A output is used as input to the Field Point Potential subprogram (PUF3FPP) [11], [12]. Calculations were then made to convert the free space potentials to pressures on the afterbody.

2. STATEMENT OF THE PROBLEM

The unsteadiness of propeller blade forces is caused by the changes in angle of attack as the propeller (Figure 1) revolves through the circumferentially non-uniform inflow field (Figure 2) (hereafter called wake field) created by the ship's hull. The hull and appendages add radial and tangential velocity components to the axial flow entering the propeller, causing the excitation forces. The inflows at the propeller plane represented by Figures 2 and 10 show vectors resolved from these two components minus the circumferential mean velocity. Another force is created by the effect of the blade's thickness and lift as the propeller rotates. At a fixed point in space, this force will be felt as a periodic pressure fluctuation of a frequency equal to blade rate and its higher order harmonics. These forces combine to form a pressure field around the ship's afterbody. The propeller rotation also induces wake velocity changes which affect the pressure field.

Another cause of pressure pulses is the rise and collapse of cavitation bubbles. These are caused by a drop in the local fluid pressure below its vapor pressure and increase the amplitude and unsteadiness of the pressure field. Much of the work in this area had its beginning in the simpler non-cavitating case. This paper examines the non-cavitating case.

3. SURVEY OF METHODS

A literature survey was conducted to identify a technique for the solution of the unsteady hull pressures produced by a non-cavitating propeller. Most of the current work has been done in the area of cavitating propellers. This work has its basis in non-cavitating flows and builds on this to represent the effects of cavitation. The survey was highlighted by four computer programs developed by Massachusetts Institute of Technology (MIT) [9], Steven's Institute of Technology, (Davidson Lab) (SIT) [13], Institute of Fluid Flow Machinery, Gdansk, Poland [14] and The Italian Ship Research Center, Genoa, Italy [15]. These four codes are based on lifting surface theory.

Two analytical techniques from Mitsubishi Heavy Industries [16] and Nippon Kokan [17], both of Japan, have been used as quick tools in the preliminary design phase of a propeller. In this phase, specific data are not known about the dimensions and operating characteristics of the full scale vessel. The information needed at this point is a rough estimate of the magnitude of the unsteady pressures that might be incurred. The first method uses the lifting surface theory and the second an empirical formula. Their accuracies are suspect due to many assumptions and empirical corrections.

3.1. Massachusetts Institute of Technology

The most promising computer program is the Propeller Unsteady Force code (PUF-3A) developed at MIT. The PUF-3A code uses the lifting surface theory and extends the vortex elements into the transition wake region downstream of the blades. Then the elements are assumed to merge into line hub and tip vortex systems. When needed, the vapor cavity source elements are extended into the transition wake region. The program is further outlined in Section 4.

3.2. Steven's Institute of Technology (Davidson Lab)

The method developed by SIT uses lifting surface theory. The main difference from the PUF-3A program is in the way the flow into the propeller is handled. In the MIT program, a known wake velocity distribution is entered as data into the program. In SIT's version, the input flow to the propeller is calculated from the interaction of a non-uniform potential flow and a hull represented by a distribution of sources. A separate computer program provides the strengths for these sources based on the shape of a hull form.

The program is general and is applicable to any propeller and hull of arbitrary form. However, it requires that the hull be subdivided into a large number of

quadrilaterals in order to obtain accurate and reliable results. Since the propeller induced velocity field is generally spatially oscillatory in character, the dimensions of each quadrilateral must be such as to fit at least four of them into one cycle of oscillation. In addition, the normal velocity to each quadrilateral requires the evaluation of three velocity components for all possible combinations of frequencies of loading with those of the propagation functions. This part of the program is the most time consuming. The excessive number of quadrilaterals makes this numerical method impractical. A new method to represent the hull sources as doublets should reduce the computation time and increase the accuracy of this technique.

From an analytical standpoint it would seem to have an advantage over the MIT approach, but with its large computation time and errors, coupled with the assumptions introduced by potential theory, this is not the case. For the PUF-3A program, results are only as good as the accuracy of the model hull wake data.

3.3. Institute of Fluid Flow Machinery, Gdansk, Poland

This method also uses the lifting surface theory. It has the requirements that propeller geometry and hull wake be known and used as irput data. The program differs from

the others in its treatment of the effects that the propeller wake has on the hull exciting forces. In particular is the geometry of the free vortex surfaces which extend behind the propeller and induce velocities on the blades.

It is assumed that the propeller wake is formed by helical vortex surfaces. The number of these surfaces equals the number of blades. The contraction effect is not taken into account, therefore the outer diameter of the wake is equal to that of the propeller. The propeller wake is divided into two zones: the so called variable zone, which contains the first complete revolution of the helices, and the steady zone, which extends further downstream, theoretically to infinity, in practice up to six revolutions of the helices. All helical surfaces inside the variable zone are then subdivided into several sectors that are equal to the number of anticipated blade positions.

As the propeller blade is moving through the non-uniform wake, the flow around the blade is changing according to the wake distribution. Simultaneously the loading distribution on the blade and intensity of the trailing vortices leaving the blade are changing. The variable intensity of the free vortex surfaces behind the propeller may be regarded as a record of the history of the blade movement through the wake. This history exerts a certain effect on the contemporary situation on the blade, via induced velocities.

It is assumed that the variable intensity of the free vortex surfaces is important only in the close vicinity of the propeller. This is where the contribution to the total induced velocity on the blade is relatively large.

This method impacts the lifting surface procedure at three points. Near the beginning, the average loading distribution is solved from the kinematic boundary conditions on the key blade. After this the induced velocities are calculated from the steady part of the vortex model of the propeller wake. Focus is now turned to the key blade where the current distribution of the local inflow velocity is interpolated. The next step is to calculate the velocities induced by the current vorticity distribution in the variable zone. The last step added is to update the vorticity distribution in the variable zone after the pressure distribution on the blade is calculated.

The method has been tested using models for the cavitating case with good results for blade rate frequency but not for higher harmonics.

3.4. Italian Ship Research Center, Genoa, Italy

This method also uses the lifting surface theory and primarily handles cavitating conditions. The main contributions of this work are the existence of empirical scale factors between model tests and full scale and the

separation of the effects of the propeller unsteady pressures from the vibrations of the hull plating at the transducers.

The investigators found that the differences between model and full scale data are due to Reynold's number effects. The wake scale factors are derived empirically and incorporated into the program to account for the differences. The results were not very satisfactory and more work needs to be done on boundary layer flow and its interaction with the propeller flow.

Previous work has been done to model the influence of the hull plating vibration on the measurements of unsteady hull pressures. This work was done independently and not integrated into any computer program. Engineers conducted reciprocity tests at full scale with a ship at rest over a range of frequency many times the blade rate. A rotating unbalanced weight was put in the superstructure as the exciting force and vibration levels over the propeller were measured with accelerometers. This level was then subtracted from vibration levels recorded at speed while taking unsteady pressure readings. The results were incorporated with the known properties of the pressure transducers and their measurements to quantify the influence of the vibrations. This information was used to make an empirical correction factor to the model and full scale data. The model and full scale calculation results were in

agreement only for the blade rate frequency.

3.5. Mitsubishi Heavy Industries, Japan

This approach finds an equation for the pressure as a function of position (cylindrical coordinates) and time, starting from a velocity potential for the blade loading and thickness. It starts with the assumption of a potential flow situation. The blade loading velocity potential is expressed with a vortex distribution on the blade. The thickness velocity potential is represented by a source distribution along the blade chord. After integration, their sum yields the pressure fluctuation induced by a non-cavitating propeller.

This technique assumes that the hull is a flat plate above the propeller, and its wake is known axially and tangentially but not radially. The pressure is multiplied by a solid body factor of 2 which represents the effect of the hull surface. The pressure calculations are for a free field and this factor comes from an imaging process where the propeller has an equal and opposite image on the other side of the hull surface. This is what gives the effect of a hull on the solution.

This technique was validated in a Norwegian water tunnel experiment. It was found that the experimental results were not affected by tunnel wall pressure reflections. The

authors presented results for the cavitating case on full scale ships, but not for the non-cavitating one. They claim to have gotten good results for the blade rate harmonic but not for any higher ones. The technique has some merit as a quick look at the blade rate pressures for trend type information. This technique does not meet the needs of a research and design program.

3.6. Nippon Kokan Inc., Japan

The approach taken by Nippon Kokan was to use full scale ship data to determine a formula for the change in pressure at the hull. For the non-cavitating case, the equation is a function of: seawater density, propeller RPM, distance from the blade at a radius ratio of r=0.9 to the hull, radius and diameter of propeller, number of blades, and empirical factors.

The authors claim that the technique is accurate for the first two blade harmonics only. The full scale ship was a tanker configuration. This formula makes no allowances for the shape of the hull and its wake, the effects of a free surface or the shape of the propeller blades.

The formula is meant to be used as a preliminary design tool. In this role, it may have some value as an order of magnitude estimate of the pressures, but it can not be used as an analytical tool for any kind of in-depth analysis.

4. PROPELLER UNSTEADY FORCE PROGRAM, PUF-3A

4.1. The Rotating Propeller as Represented by Lifting Surface Theory

The PUF-3A code uses the lifting surface theory. This theory is the basis for a procedure where a propeller blade is represented by a lattice of discrete line vortex and source elements located on the mean camber surface of the blade. Sources are used to represent the thickness of the blade profile. The sources are independent of time and their spatial distribution is derived from a stripwise application of thin wing theory at each radius. The problem is formulated with many assumptions:

1. The blade/propeller is fully wetted and the flow is potential.
2. The hull wake velocity components (axial, radial and tangential) are known at any given time.
3. The blades are all symmetrical, rotating on a common axis with constant angular velocity in the clockwise direction looking forward (right hand convention).
4. Effects due to the propeller hub and the rudder are neglected.
5. The total velocity can be divided irto the ship wake and a propeller perturbation velocity.
6. The blade boundary layer and shed vortex wake thickness are assumed to be thin so that the fluid

rotation due to the propeller is confined in a thin layer.

The vortex lattice system provides the circulatory flow responsible for the lift on the blades. It represents the jump of the tangential velocity both at the camber surface and in the trailing wake sheet. The vortex strength is a vector lying on the surface and may be resolved into components along two arbitrarily assigned directions on the surface. The vortex distribution on the blade will be resolved into "spanwise" and "chordwise" components while the corresponding components (Figure 3) in the wake will be termed "shed" and "trailing" vorticity. The vortex elements extend into the transition wake region downstream of the blades. These elements are assumed to merge into line hub and tip vortex systems (Figure 4).

The vortex strength is determined as a part of the solution to this boundary value problem. The solution will also satisfy the conservation of mass principle. There are four boundary conditions for the non-cavitating case:

1. Quiescence Condition: At an infinite distance upstream the perturbation velocity due to the propeller vanishes.
2. Tangency Condition: The fluid can not pass through the surface of the blades.
3. Kutta Condition at Trailing Edge: Velocity at the trailing edge will be finite.

4. Kinematic and Dynamic Wake Conditions: The velocity increase must be purely tangential to a shed vortex wake sheet and the pressure must be continuous across this vortex wake sheet.

The application of these boundary conditions will lead to coupled integral equations. One solution of these equations is to discretize the boundaries and satisfy the boundary conditions on the selected collocation points. This will result in a set of simultaneous equations for the determination of the vortex and source strengths.

The continuous distribution of vortices and sources are replaced by a lattice of concentrated straight line elements of constant strength for the purpose of digital computation. This enables the velocity induced at any point in space by these line source or vortex elements to be computed.

The most critical step in developing a numerical lifting surface theory is to find the lattice arrangement which is optimum in providing answers to the desired accuracy with a minimum number of elements. For a non-cavitating propeller it has been found that the best arrangement of elements is one that has uniform intervals in the chordwise and radial directions.

These conditions describe one blade on the propeller. A computational economizing technique is used where one blade is called the key blade and the strengths of the sources and vortices on the other blades are known in terms of the

corresponding values on the key blade at a previous time step. Computational time is reduced if the number of elements on the other blades is a submultiple of the key blade. This permits the concentration of the strengths of several elements on the key blade into a single element on the other blades.

The stepwise solution method is employed for the solution of the boundary value problem in the time domain, in which the results from the key blade are used to update the strengths of sources and vortices on the remaining blades. This happens while trailing and shed vortices are being convected downstream to account for propeller advance.

The key blade is oriented at an angle with respect to a coordinate frame fixed on the ship. The relative inflow velocity, the velocity induced by the sources representing the blade thickness, and the velocity induced by the vortex elements on the remaining blades and in the wake are combined to produce an effective inflow seen by a one-bladed propeller. The simultaneous equations are solved for the unknown strength of the spanwise vortices on the key blade at the present time. As the process is repeated, the circulation strengths on the other blades are updated.

4.2. Program Inputs

The PUF-3A program and PUF3FPP subprograms have three main input files; propeller geometry, ship wake data, and field point location. The propeller geometry file incorporates the parameters of pitch, chord length, camber, rake, thickness, and skew by the nondimensional radius ratio as shown in Appendix A. Appendix E. defines the hydrodynamic parameters of advance ratio, cavitation index, and Froude number, and specifies these and other parameters for the water tunnel tests.

The wake survey describes the water velocity at radial stations, before the propeller plane, in terms of vector components in an axial, radial, and tangential coordinate system. Each velocity is then non-dimensionalized by the ship free stream velocity to form a wake component. The wake input file contains the coefficients of a harmonic series that describes the curve created by each velocity component versus its angular position. Examples are shown in Appendix B. and Appendix C. for the normal and modified wakes (Figures 5 and 6), respectively.

The field point input file gives the axial, radial, and circumferential positions of the free field points to be evaluated. An example is provided in Appendix D.

4.3. Program Parameters

The PUF-3A and PUF3FPP programs have four main parameters that set internal conditions for the solution. These are based on the degree of accuracy and the running time desired. The first three are switches given in the propeller input file for PUF-3A, while the fourth is in the PUF3FPP subprogram.

1. NPROP (1 or 2) - Controls the number of spanwise cavity iterations at each angular position of the propeller blade.
2. MXREV (4 or 7) - Specifies the number of computational revolutions of the propeller. These choices are for the unsteady case in cavitating or non-cavitating modes.
3. NN (10 or 20) - This is the number of chordwise lattice elements on the key blade. An input of 20 gives higher accuracy and lower speed.
4. NUW (50 or 100) - This is the number of streamwise panels used to calculate the effect of the propeller wake on the solution.

The program was exercised with 16 different combinations of the paramters for the same propeller geometry, ships wake field and hull transducer locations. The sound pressure levels at the field points were graphed for the first three blade rates. It was found that six combinations gave

discernible differences. These differences were mainly found in the second and third blade rates. The six combinations were compared to the water tunnel results for a best fit. The combinations were run again for two different wakes and compared to water tunnel results.

4.4. Field Point Potential and Pressures

The Field Point Potential subprogram [12] PUF3FPP, computes the amplitudes of the velocity potential function at arbitrary field points due to the influence of a propeller working in a non-uniform wake field. The potentials are for a free field with the propeller wake, loading, and thickness taken into account.

The program takes two inputs from PUF-3A. The first contains the coordinates of the vortex and source line elements in the lattice on the key blade and the strengths of the time independent sources representing the blade thickness. This input is for the key blade and in the transition and ultimate wake of this blade. The second input contains the loading source strengths for the sixty time steps that describe one revolution of the propeller.

The area, center, and components of the unit vector normal to each quadrilateral lattice panel are then calculated using geometrical techniques. The individual vortex lattice panel strength is then multiplied by the area

of its panel to yield the point dipole strength. The program sums the strengths of the dipoles and sources and gives the potential at a single field point.

The dipole potential is expressed by Kerwin and Greeley [12] as;

$$\Phi = \frac{-1}{4\pi} \frac{(X_f-X_s)X_n + (Y_f-Y_s)Y_n + (Z_f-Z_s)Z_n}{[(X_f-X_s)^2+(Y_f-Y_s)^2+(Z_f-Z_s)^2]^{3/2}} \qquad (1)$$

The source potential is given by [12];

$$\Phi = \frac{-1}{4\pi} [(X_f-X_s)^2+(Y_f-Y_s)^2+(Z_f-Z_s)^2]^{1/2} \qquad (2)$$

The field point locations are input and the program performs a harmonic analysis of the potentials through a revolution of the propeller. The results are the amplitude and phase of the velocity potential function at a field point. For the case of a five bladed propeller, the function is calculated for the first three blade rates.

The pressures are then calculated from [18];

$$P = \frac{2\pi\rho}{gc} \cdot \Phi \cdot \frac{n^2 D^2}{1000} \cdot SBF \qquad (3)$$

Equation (3) non-dimensionalizes the potential and introduces the "Solid Body" factor. The SBF takes into account the shape of the hullform being evaluated. The range is from one for a "Vee" type hullform to two for a block or tanker type hullform.

5. EXPERIMENT

The experimental data was obtained for the two propeller configurations described in this paper. The tests were performed in the Applied Reasearch Laboratory's 48-inch diameter water tunnel (Figure 7). Figure 8 shows the test configuration with the section of the ship hull that is below the water line mounted in an inverted position on a splitter plate in the tunnel test section. The propeller was powered by two internal 20-hp motors on the model shaft. There were five unsteady pressure transducers laid out transversely on the hullform in the propeller plane (Figure 9). The measurement points extended from the centerline transversely to a distance about 1.4 times the propeller radius. To simulate the correct wake into the propeller, the locally modeled shaft and bossing were set at an inclination angle of 7.5 degrees to the tunnel centerline. Model hull to blade clearances were kept consistent with full scale construction. Flow parameters such as cavitation number, advance ratio, and gas content were maintained so as to be consistent with full scale.

A powered wake survey was performed in the plane of the propeller to determine the circumferential distribution of the axial, radial, and tangential velocity components (Figures 5 and 6). During the measurement of the nonuniform inflow, the propeller was driven with a downstream shaft

arrangement in the tunnel. The ship shaft was used to incrementally step the wake rake. The velocity components were measured by a rake of six five-hole pressure probes with the propeller being powered by a dynamometer. This method is important because the effects of the propeller on the hull and shaft wake are taken into account. Two different wakes were studied with the same propeller. The first wake (Figure 2) was for a standard hull and shaft barrel configuration. The second configuration used reaction fins placed on the barrel and struts to place counterswirl in the flow to offset the oblique inflow to the propeller due to the shaft inclination [19]. The wake for the second configuration is shown in Figure 10.

6. RESULTS

The results of the water tunnel tests and the PUF-3A program were reduced to curves of the sound pressure level (SPL, dB re 1μPa) versus the transverse distance from the keel on the hull model for the first three harmonics of blade rate. The potentials from PUF-3A were converted to pressures using Equation (3) and then transformed to SPLs in decibels. The decibel values were fit with a cubic spline routine to form the curves.

With hull mounted pressure transducers outside the transverse distance of the propeller radius, the outer edge effects can be examined. The water tunnel data for the outer edge were well behaved. This was expected because the model configuration had a flat plate where the waterline, air/water boundary, would be for an actual ship. The PUF-3A data were almost as well behaved because it does not model the water line's free surface or pressure release effects. These effects tend to lower the pressure fluctuations in this region. For this reason, predictions of full scale results at larger transverse distances from the centerline will be increasingly inaccurate. The SBF is an attempt to empirically correct for these effects. A value of two was used because the model hull was closer to a tanker type hullform in shape than a "Vee" type hullform.

The water tunnel experiments showed that the first blade

rate harmonic was dominant when compared to the second or third harmonics. The PUF-3A program confirmed this result. The analysis also included the addition of four extra field points between the five experimental data points. These have no correlating water tunnel data and were added to see how the program reacts. Generally these yielded higher pressures than the analyses of the actual data points. Relative to each other, these had a shape similar to the actual data.

The water tunnel data for the two propulsor configurations were compared with six combinations each of PUF-3A/PUF3FPP curves. For both wakes, the combination of parameters that gave the closest results to the water tunnel data was for the simplest case. It used the non-cavitating solution, indicating that there was no cavitation present. The spanwise cavity iteration scheme was included in case cavitation was found, but proved to have no effect. The streamwise variation in the number of wake panels had no effect indicating a well behaved wake as would occur for the non-cavitating case. The chordwise number of lattice panels did affect the shapes of the second and third blade rate curves. The higher number of panels gave a small undulation in the third harmonic of the unmodified wake. It also resulted in a higher SPL as the transverse distance increased on the starboard side in the second harmonic of the modified wake.

The program breaks down the total potential into the contributing parts of blade loading, blade thickness, and cavitation. Cavitation was not found to occur in the analysis. The blade loading and thickness are low frequency disturbances. The program does not model the high frequency disturbances caused by the interaction of shed vortices and boundary layers. This is a weakness of the program in calculating the potentials at the higher harmonics.

6.1. Comparing PUF-3A results with Water Tunnel Data for a Normal Wake

The shape of the blade rate curve obtained in the water tunnel tests (Figure 11) indicates a peak at the propeller centerline with a general decrease in SPL as the transverse distance increases. This is expected because the radial distance is the smallest and the pressure field is perpendicular to the hull form at this point. The curve was slightly higher on the starboard side near the centerline due to the right hand rotation of the propeller. The angle of attack that the blade encounters changes as it passes top dead center. The blade loading increases as does its contribution to the pressure field. The contribution then decreases as the blade continues to rotate and the distance to the field point increases. The curve is influenced most by the spatially non-uniform wake from the hull.

The PUF-3A program predicted the relative overall SPL but produced a curve (Figure 12) of slightly different

shape. It gave a lower value on the port side near the centerline and higher values at the outer points. For this fundamental harmonic, the program models the influence of the non-uniform inflow caused by the wake of the hull as larger than that of the appendages.

The program slightly over predicts the SPL at the outer edges or field points for two reasons. These outer points are relatively distant from the outermost radius of the given wake field and the flow past them is increasingly unknown. The program knows the position of the field points but not the flow field outside of the described circumferential wake at the largest radius. The SBF, in the potential to pressure calculation, tries to account for this by assigning a number to a description of the overall curvature of the hull.

The second harmonic test data (Figure 11) also reveals a peak SPL at the centerline, but with an overall relative SPL lower than the first harmonic. Its shape is flatter than the first harmonic and is characterized by a lower SPL for data on the port side near the centerline and a rise on the outer starboard side. The influence of the upstream appendages; vortices shed by the struts, wake of the barrel, and a Strouhal vortex from the rotation of the shaft, is to decrease the overall SPL and create variations near the centerline of the hull. The hull's spatially non-uniform flow has a greater influence than the wake of the appendages

at the outer field points. This harmonic has a higher SPL at the outer field points relative to the inner ones than the first harmonic.

The PUF-3A program (Figure 12) predicts the relative overall decrease in SPL from the fundamental harmonic and the predicted curve has a similar shape to the measured one. The predicted curve does not indicate the correct height of the peak in the test data at the centerline and predicts the rise in the outer starboard side SPL at a shorter transverse distance. The program does not handle the complex appendage flows very well as its results do not duplicate the variation in SPL in the region of the centerline of the hull. The results do indicate that the influence of the spatially non-uniform inflow is slightly over predicted in the outer field points.

For the water tunnel, the third blade rate test data (Figure 11) exhibits a cyclic rise in SPL from port to starboard with the maximum at an outer point on the starboard side. This could be the effect of a bilge vortex from the hull wrapping into the induced flow near the outer field point. Its overall relative SPL is slightly lower than the second harmonic. The overall results were similar to the second harmonic.

PUF-3A (Figure 12) predicts the relative SPL for this harmonic but not the rise on the starboard side. The PUF-3A curve is flat in this section. The influence of the

appendages was difficult to model and the variation in SPL in the region near the centerline of the hull was not well predicted. The program slightly over predicted the port side outer points and under predicted the starboard side. The starboard result could be the coupling of energy from vortices shed by appendages.

6.2. Comparing PUF-3A Results with Water Tunnel Data for a Modified Wake

The relative SPL of the first harmonic of the blade rate experimental curve for the modified wake is roughly equal to the level of the unmodified one. The curve (Figure 13) is characterized by a peak at the outer points and a dip at the inner points on the port side and a peak on the starboard side near the propeller centerline. At the outer points on the port side, the pressure field is dominated by the effects of the hull wake and tip vortices from the wake modifying device. These combine to increase the SPL relative to the unmodified curve for this harmonic. On the inboard port side, the wake modifying devices affect a greater portion of the propeller disk area relative to the appendages and shed their own vortices that alter the inflow. The wake modifications dominate the effects of the appendages as seen by the dip in the SPL compared to the curve of the unmodified wake for the same region. The devices increase the blade loading by altering the angle of attack. The curve rises slightly on the starboard side near

the centerline due to the right hand rotation of the propeller. The angle of attack that the blade encounters changes as it passes top dead center. The blade loading increases as does this contribution to the pressure field. The contribution then decreases as the blade continues to rotate and the distance to the field point increases.

The PUF-3A program predicted the overall SPL levels but produced a curve (Figure 14) of a different shape. It gave a lower value on the port side near the centerline and higher values at the outer points. The program seems to predict the influence of the combined hull wake and device vortices outboard on the port side. It over predicts the influence of wake modifications towards the center on the port side. It over predicts the SPL at the outer starboard side due to the same circumstances as the unmodified wake.

The second harmonic test data (Figure 13) are characterized by a peak SPL at the outer points on the port side, a decrease at the centerline, and a rise on the outer starboard side. The upstream wake modifications combine with the effects of the appendages and raise the overall SPL above the corresponding harmonic for the unmodified wake. This was expected because the modifying devices shed their own vortices that alter the inflow creating more unsteadiness. The spatially non-uniform inflow from the hull still dominates the flow at the outer field points. This harmonic has a high SPL at the outer field points like the

unmodified case.

The PUF-3A (Figure 14) program over predicts the relative decrease in SPL for the second harmonic. The program seems to shift the low point of the curve to the port side. It does not indicate the correct height of the peak in the test data at the centerline and predicts the rise on the outer starboard side SPL at a shorter transverse distance. The program did not handle the combined complex appendage and wake modification flows very well as the results do not duplicate the variation in SPL in the region of the centerline of the hull. The results do indicate that the influence of the spatially non-uniform hull inflow is handled correctly in the outer field points.

The third blade rate of the test data (Figure 13) exhibits a dip on the port side rising to a peak on the starboard side similar to the first blade rate harmonic. The appendages and upstream wake modifications on the port side combined to increase the unsteadiness. The centerline variation in SPL was less than the variation for the unmodified wake. Its overall relative SPL is slightly lower than the second harmonic and higher than the third harmonic of the unmodified wake. The PUF-3A (Figure 14) program over predicts the relative decrease in SPL for the third harmonic,but predicts the SPL in relation to the second harmonic. The flat curve exhibits no clear influence of any of the physical parameters of the problem.

7. SUMMARY AND CONCLUSIONS

Several computer programs were examined and PUF3A appeared the most promising. It was the most versatile because it looked at individual components of the physical problem, such as the effects of blade loading and thickness and cavitation.

The program's strengths were in predicting the relative SPLs versus distance across the hull of the first blade rate harmonics in the two different wake fields. In the simpler case of the unmodified wake field, the relative SPLs of the second and third harmonics compare reasonably well with water tunnel data. The low frequency disturbances of blade loading and thickness are modeled while the high frequency disturbances caused by the interaction of shed vortices and boundary layers are not. This shows up as a strength in calculating blade rate SPLs for simple wake fields, but as a weakness for calculating SPLs at the higher harmonics in complex wake fields.

The main weaknesses of the program are that it is based on a potential flow approach with its hydrodynamic assumptions of blade similarity, thin boundary layers and lack of viscosity and vorticity. The water tunnel data taken with the modified wake indicated a more complicated flow near the center of the propeller. For this case, the program did not predict the overall increase in SPL for the

second and third harmonics. The limitations of the program increase with the complexity of the flow field. The complexities in this case are shed vorticies from the appendages interacting with the hull wake, and all phenomena being influenced by the effects of the propeller.

These real factors must be modeled before accurate solutions can be obtained for complex wake flows. The PUF3A program is a useful tool for a first cut prediction of blade rate hull unsteady pressures for most wake fields. For a simple wake field, the overall sound pressure levels for the second and third harmonics, relative to blade rate, can be reasonably predicted.

REFERENCES

1. Breslin, J. P., "Theory for Vibrating Effects Produced by a Propeller in a Large Plate", Journal of Ship Research, Vol. 3, No.3, 1959.

2. Breslin, J. P., "Review and Extension of Theory for Near Field Propeller Induced Vibratory Effects", Fourth Symposium on Naval Hydrodynamics, Washington, D. C., 1962.

3. Vorus, W. S., "A Method for Analyzing the Propeller Induced Vibratory Forces Acting on the Surface of a Ship Stern", Transactions, The Society of Naval Architects and Marine Engineers, New York, Nov. 1974.

4. Huse, E., "The Magnitude and Distribution on Propeller Induced Surface Forces on a Single Screw Ship Model", Norwegian Ship Model Experiment Tank Publication No. 100, December, 1968.

5. Jacobs, W., Mercier, J., and Tsakonas, S., "Theory and Measurements of the Propeller Induced Vibratory Pressure Field", Journal of Ship Research, Vol. 16, No. 2, June, 1972.

6. Holden, K. O., Fagerjord, O., and Frostad, R., "Early Design Stage Approach to Reducing Hull Surface Forces Due to Propeller Cavitation", Transactions, The Society of Naval Architects and Marine Engineers, New York, November, 1980.

7. Kerwin, J. E. and Lee, C. S., "Prediction of Steady and Unsteady Marine Propeller Performance by Numerical Lifting Surface Theory", Transactions, The Society of Naval Architects and Marine Engineers, New York, Vol.86, 1978.

8. Lee, C. S., "Prediction of the Transient Cavitation on Marine Propellers by Numerical Lifting Surface Theory.", 13th Symposium on Naval Hydrodynamics, Tokyo, Japan, October, 1980.

9. Kerwin, J. E., "A Numerical Method for the Analysis of Cavitating Propellers in Nonuniform Flow", MIT-PUF3A User's Manual (revised edition), Technical Report 90-3, MIT, Department of Ocean Engineering, January, 1990.

10. Kerwin, J. E., "A Numerical Method for the Analysis of Cavitating Propellers in Nonuniform Flow", MIT-PUF3A Documentation and Listings (revised edition), Technical Report 90-4, MIT, Department of Ocean Engineering, January 1990.

11. Kerwin, J. E., and Greeley, D. S., "A Numerical Method for the Calculation of Field Point Potential due to a Cavitating Propeller", MIT-PUF3FPP User's Manual (revised edition), Technical Report 90-5, MIT, Department of Ocean Engineering, January, 1990.

12. Kerwin, J. E., and Greeley, D. S., "A Numerical Method for the Calculation of Field Point Potential due to a Cavitating Propeller", MIT-PUF3FPP Documentation and Listings (revised edition), Technical Report 90-6, MIT, Department of Ocean Engineering, January, 1990.

13. Tsakonas, S. and Valentine, D., "A Theoretical Procedure for Calculating Propeller Induced Hull Forces", Davidson Laboratory, Hoboken, NJ, report SIT-DL-79-9-1979.

14. Szantyr, J., "A New Method for the Analysis of Unsteady Propeller Cavitation and Hull Surface Pressures", The Royal Institution of Naval Architects, London, England, 1984.

15. Colombo, A. and Chilo, B., "Experimental Verifications of a Theoretical Procedure for Propeller Induced Hull Pressure Calculations", Marine Technology, Vol 21, No. 2, April, 1984, pp. 119-133.

16. Chiba, N., Sasajima, T. and Hoshino, T., "Prediction of Propeller Induced Fluctuating Pressures and Correlation with Full Scale Data", Mitsubishi Heavy Industries, Japan, 1981.

17. Ohta, T., et al, "A System for the Prediction of Hull and Superstructure Vibration at an Early Design Stage", Nippon Kokan Technical Report, Overseas No. 39, 1983.

18. Kerwin, J. E., private communication, December, 1989.

19. Gearhart, W. S. and Marboe, R. C., "Asymmetric Reaction Vane Application", Proceedings of Symposium of Hydrodynamic Performance Enhancement for Marine Applications, Newport, RI, 1988.

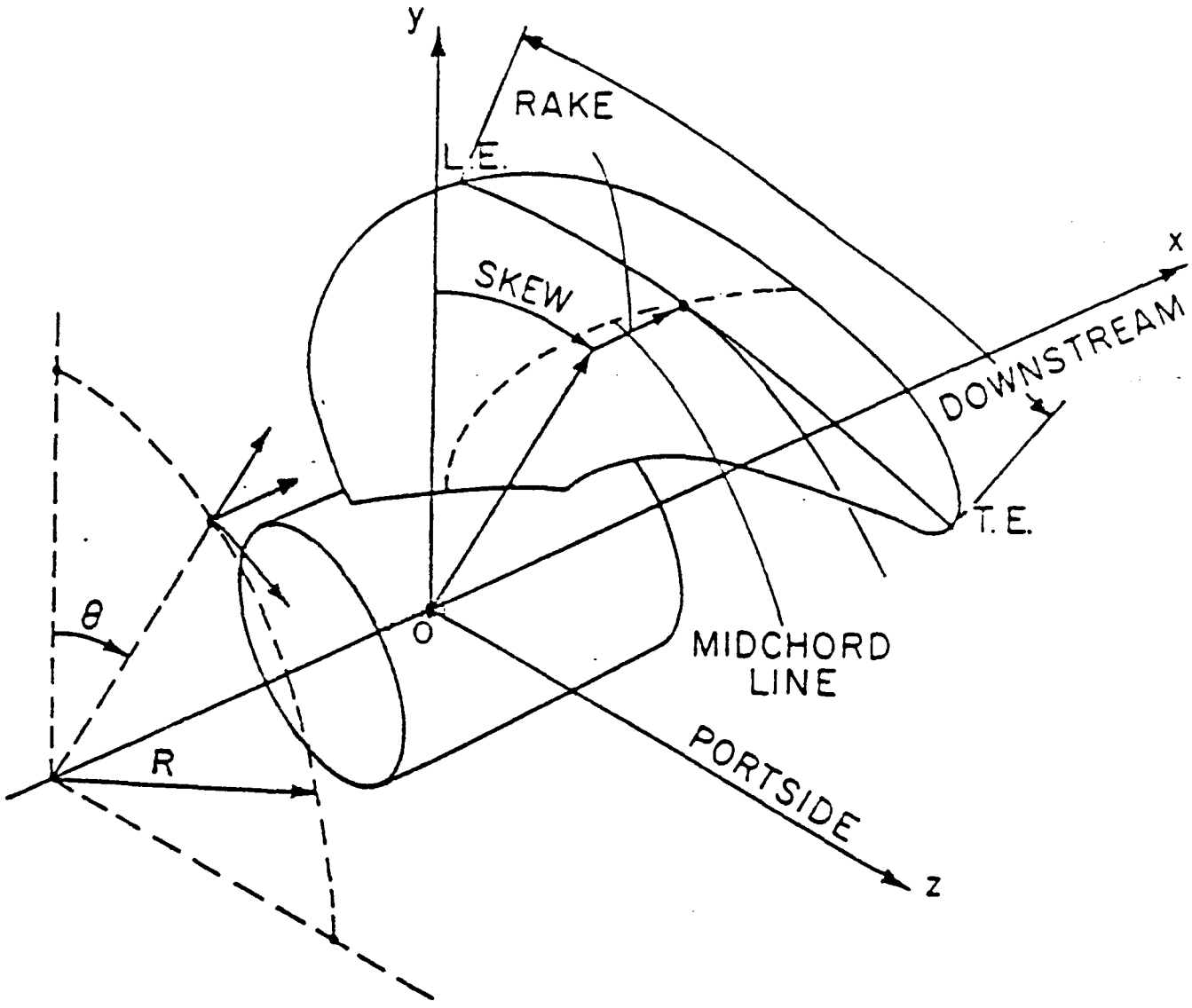

Figure 1.

Propeller Schematic

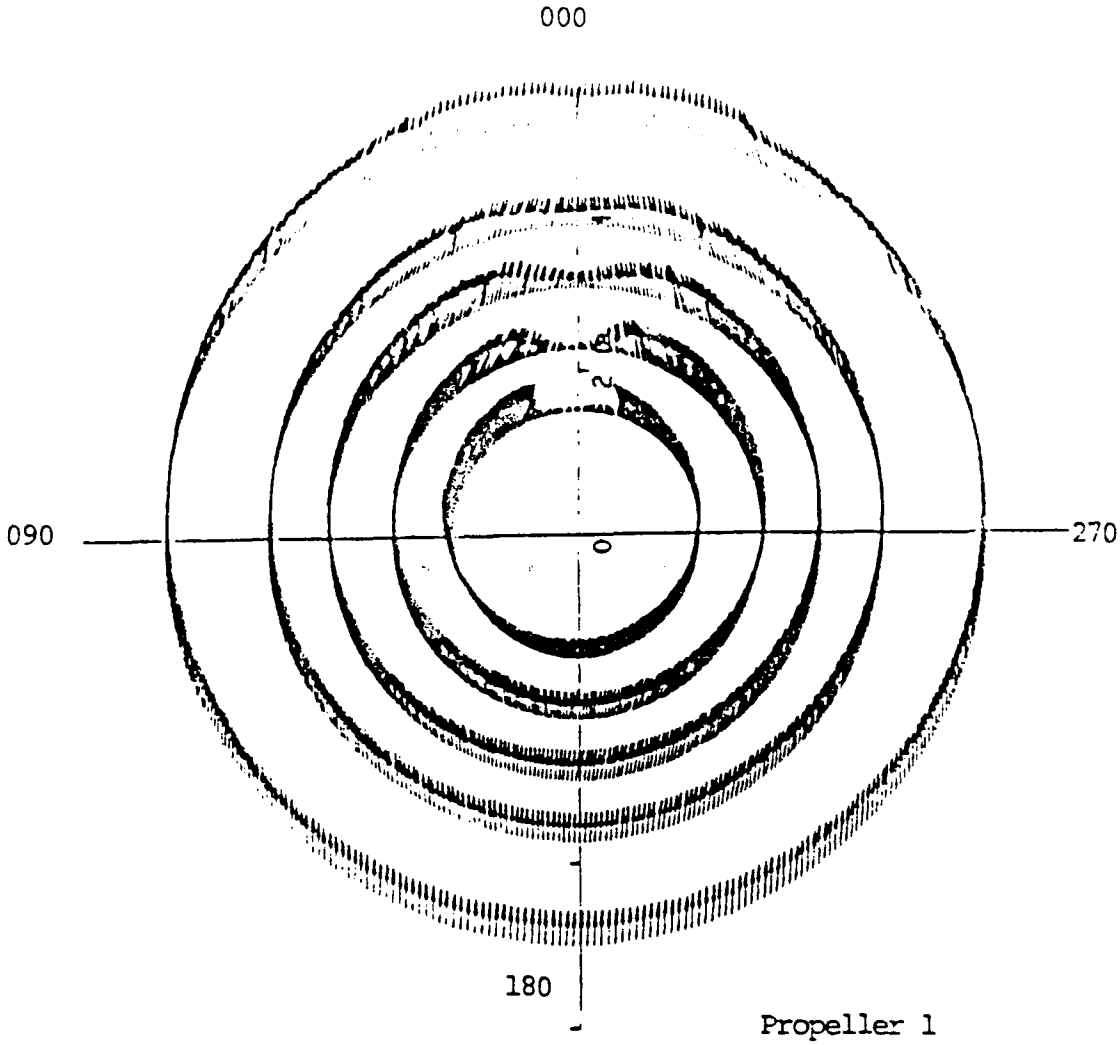

Deviations from average tangential and radial velocity in the inflow plane of the propeller.

Figure 2.

Afterbody Wake Representation

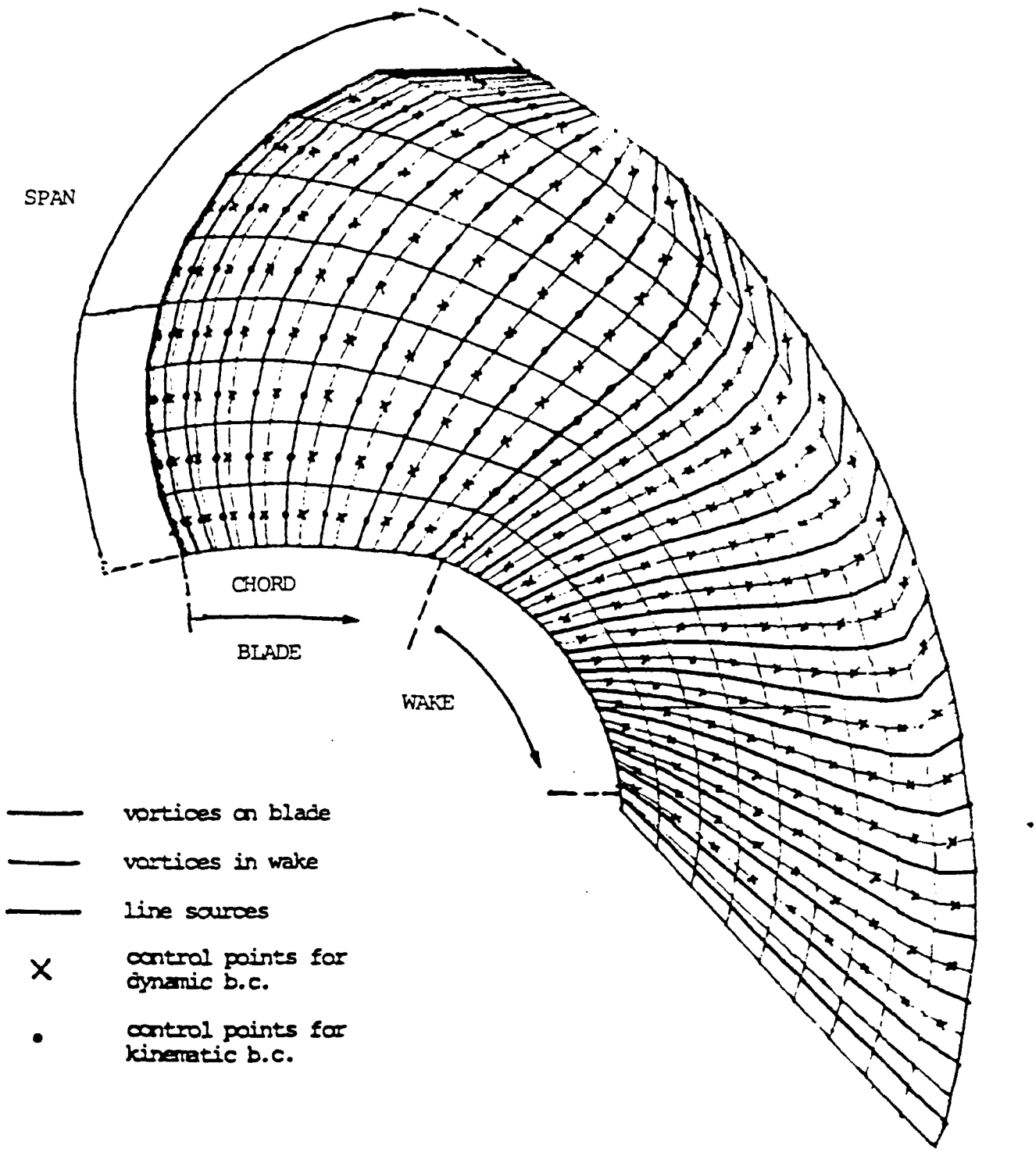

Figure 3. Grid Geometry of the Key Blade and its Wake

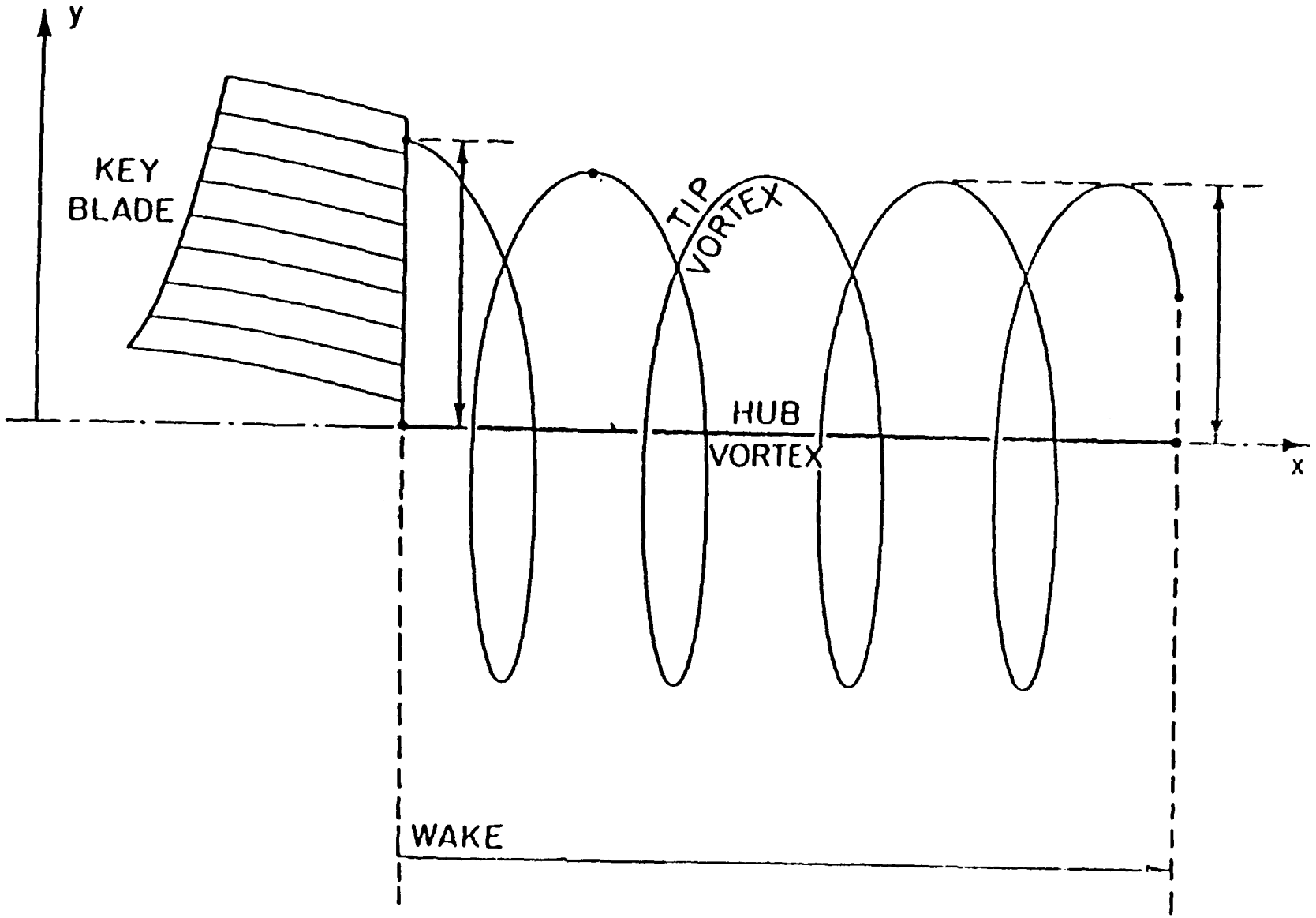

Figure 4. Line Hub and Tip Vortex System

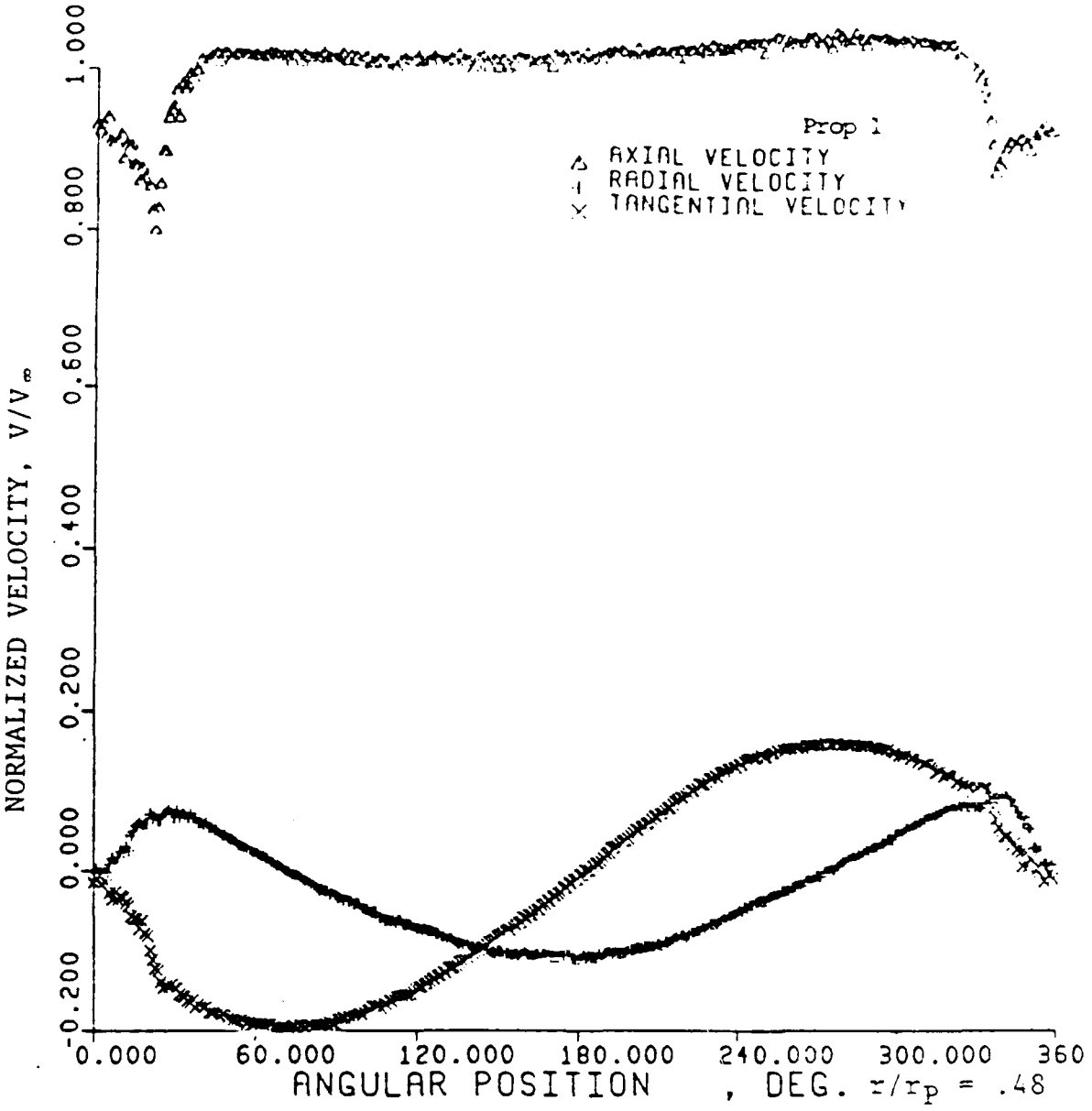

Figure 5.

Wake Survey

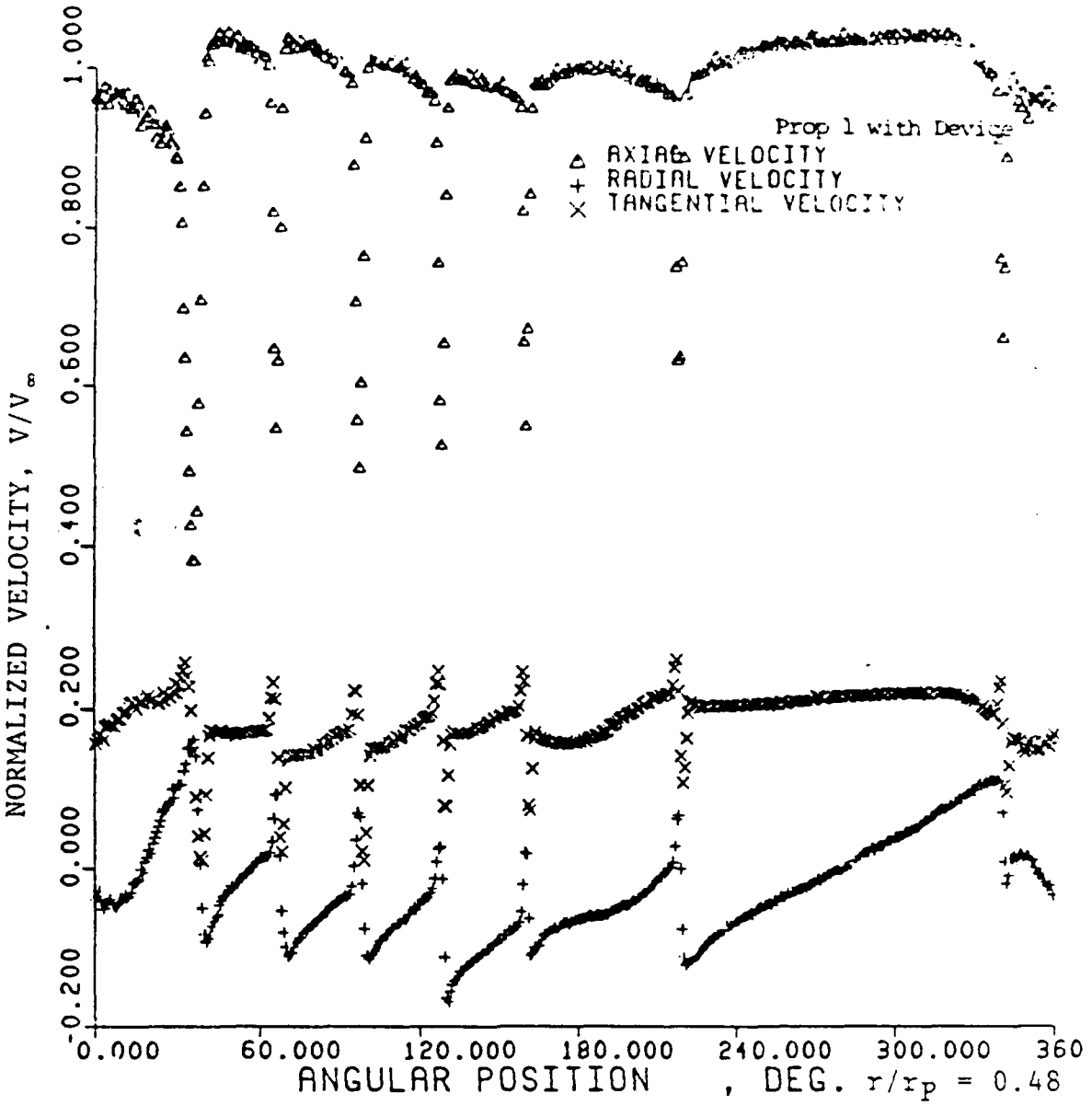

Figure 6.

Modified Wake Survey

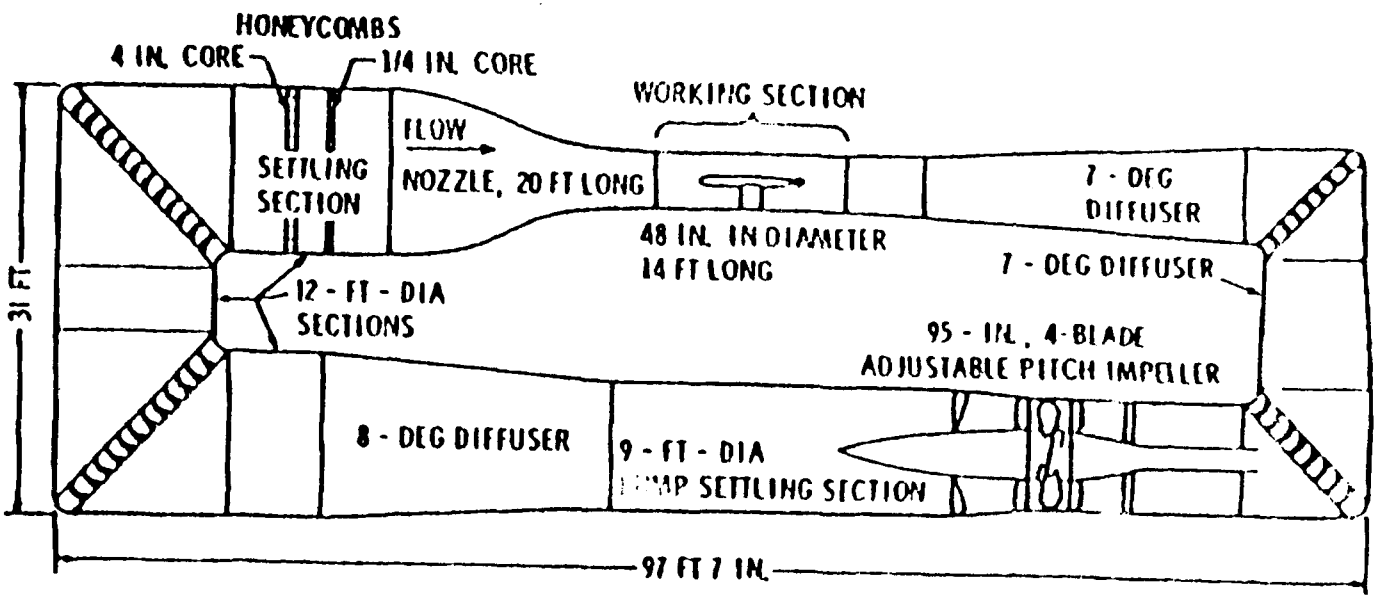

THE 48-INCH WATER TUNNEL

Figure 7.

Water Tunnel Schematic

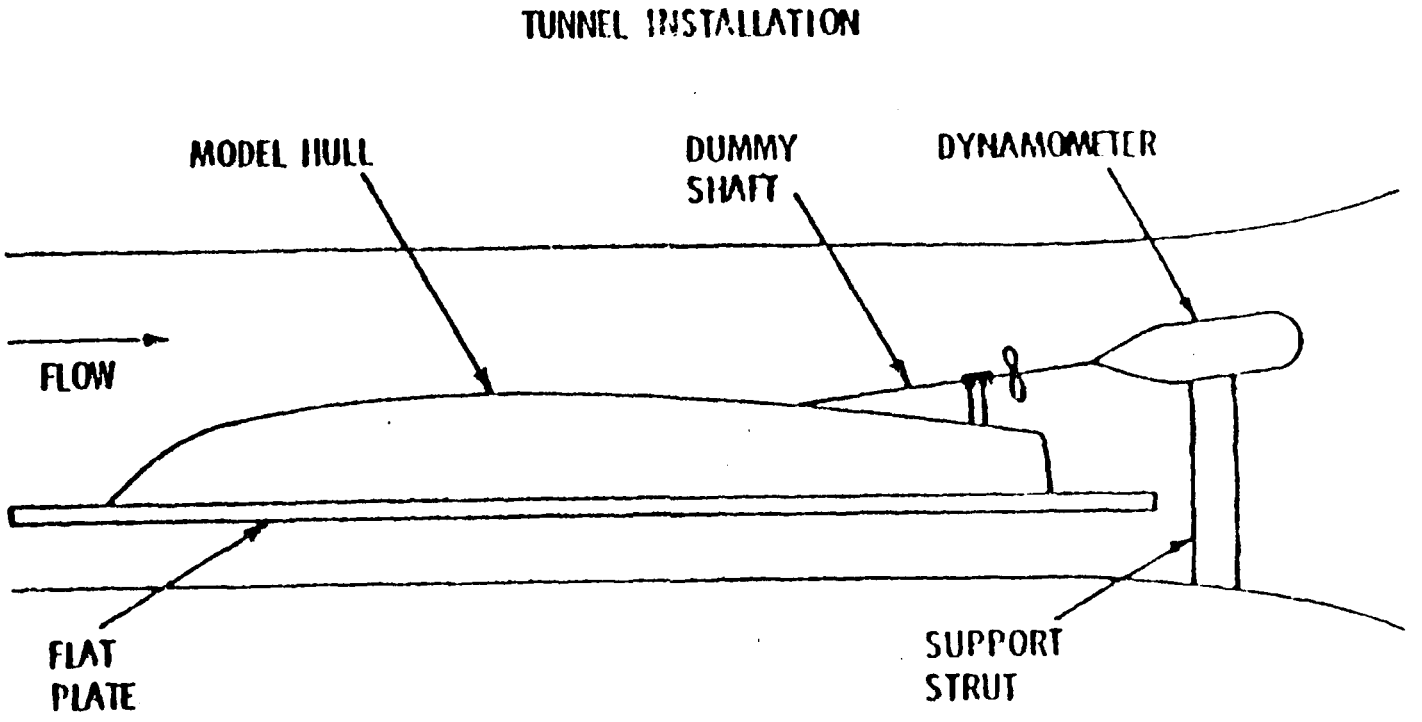

Figure 8.

Model Afterbody and Propeller Configuration

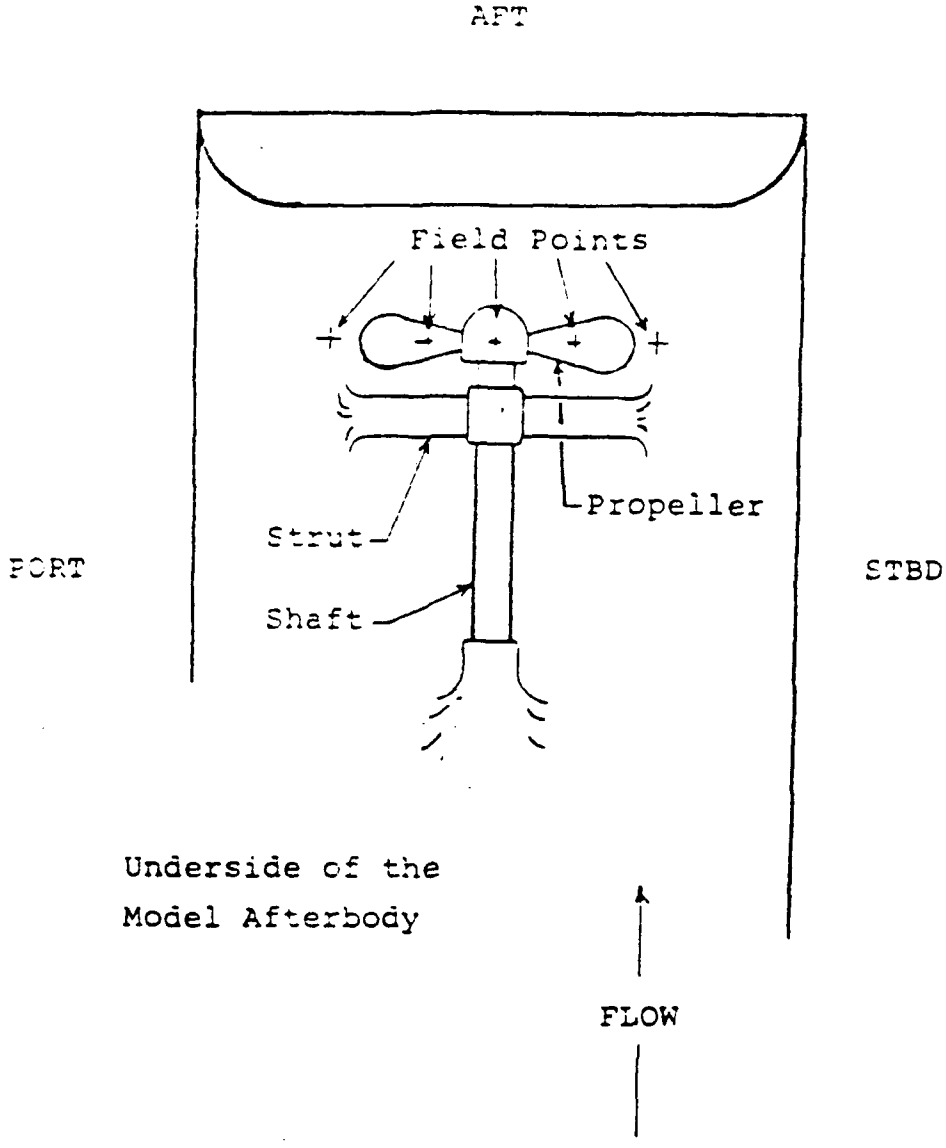

Figure 9.

Position of Field Points on the Model

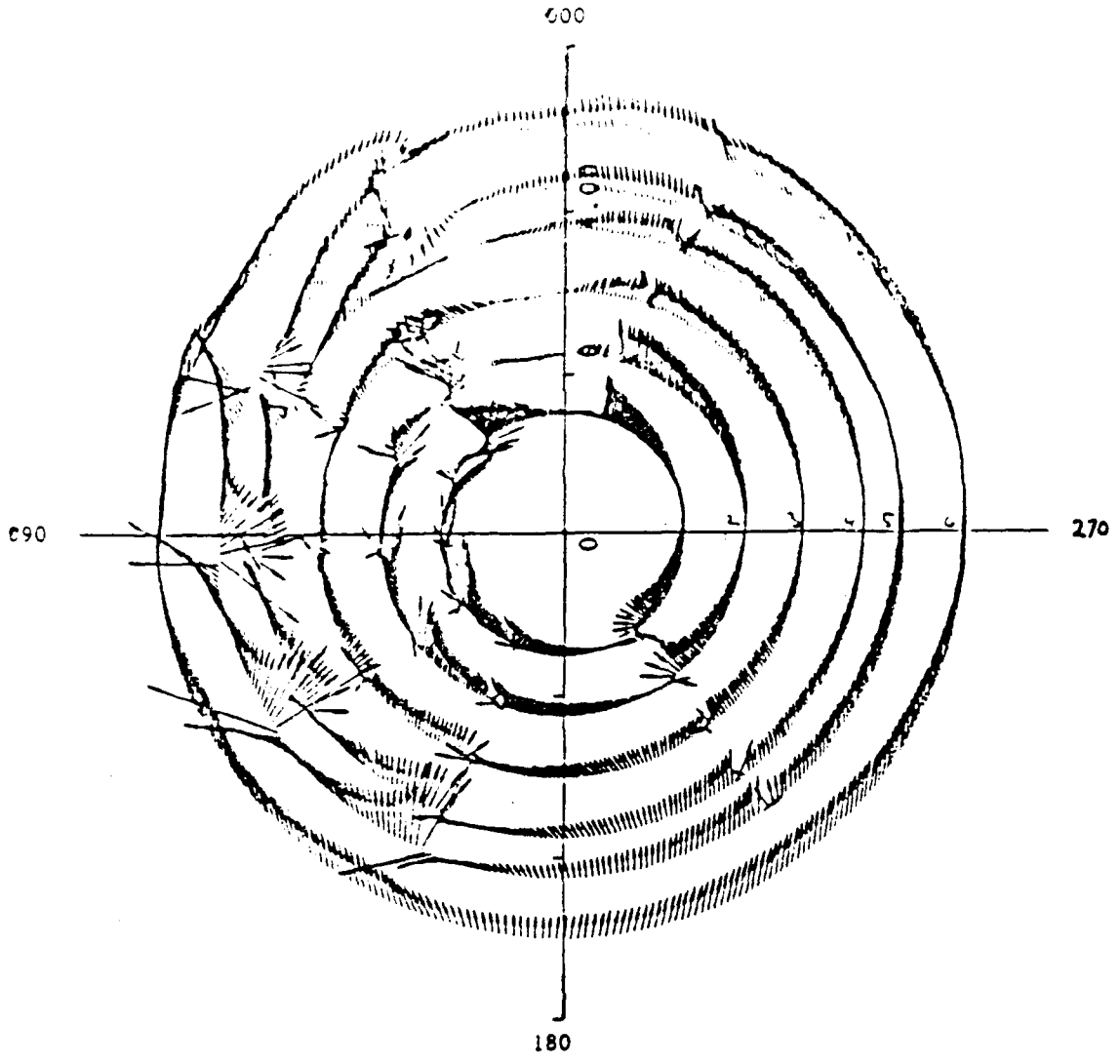

Deviations from average tangential and radial velocity in the inflow plane of the propeller.

Figure 10.

Modified Afterbody Wake Representation

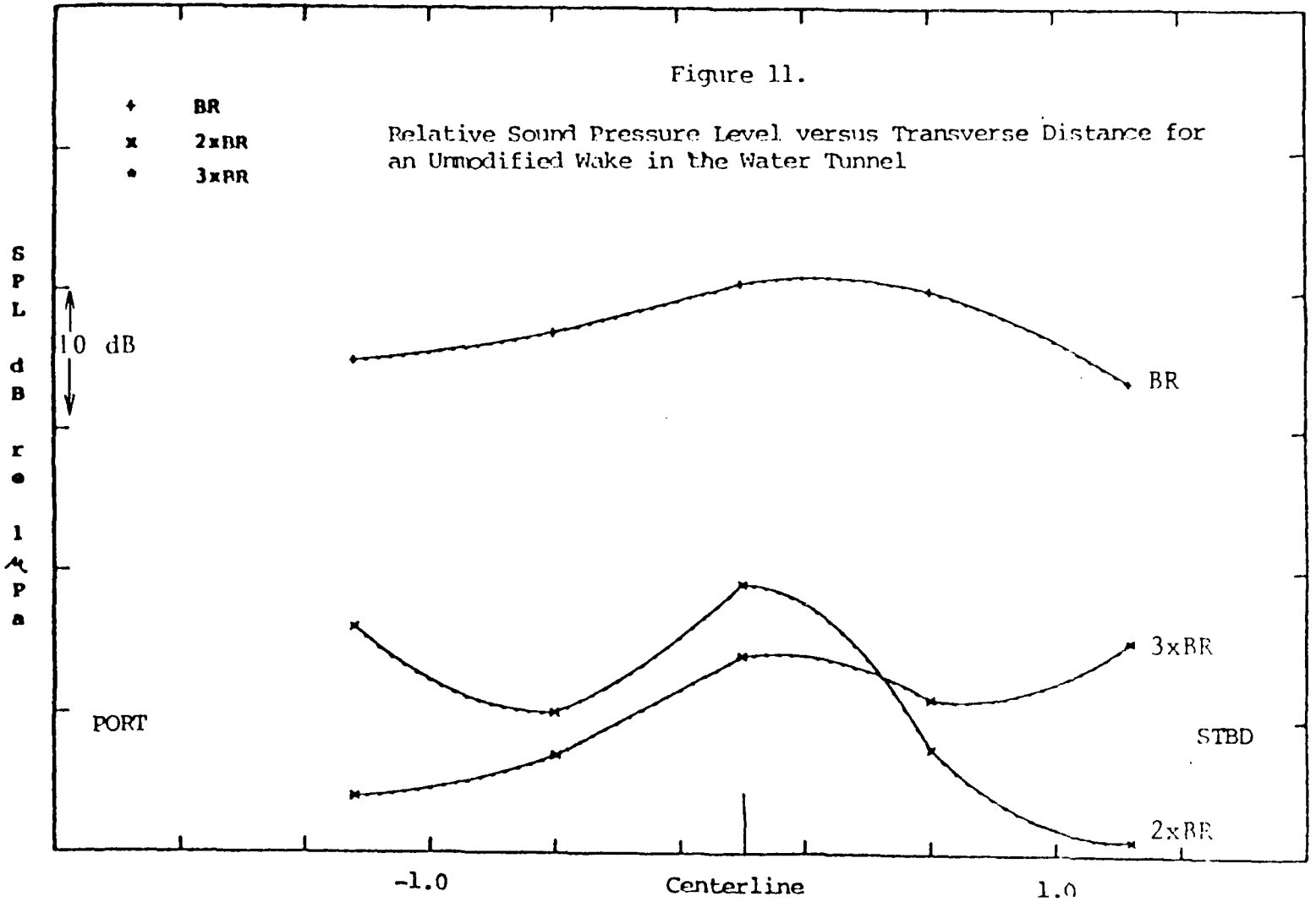
Figure 11.
BR
2xBR
3xBR
Relative Sound Pressure Level versus Transverse Distance for an Unmodified Wake in the Water Tunnel
SPL dB re 1 μPa
10 dB
BR
3xBR
2xBR
PORT
STBD
-1.0
Centerline
1.0
Transverse Distance across Hullform Non-dimensionalized by Propeller Radius

Figure 12.

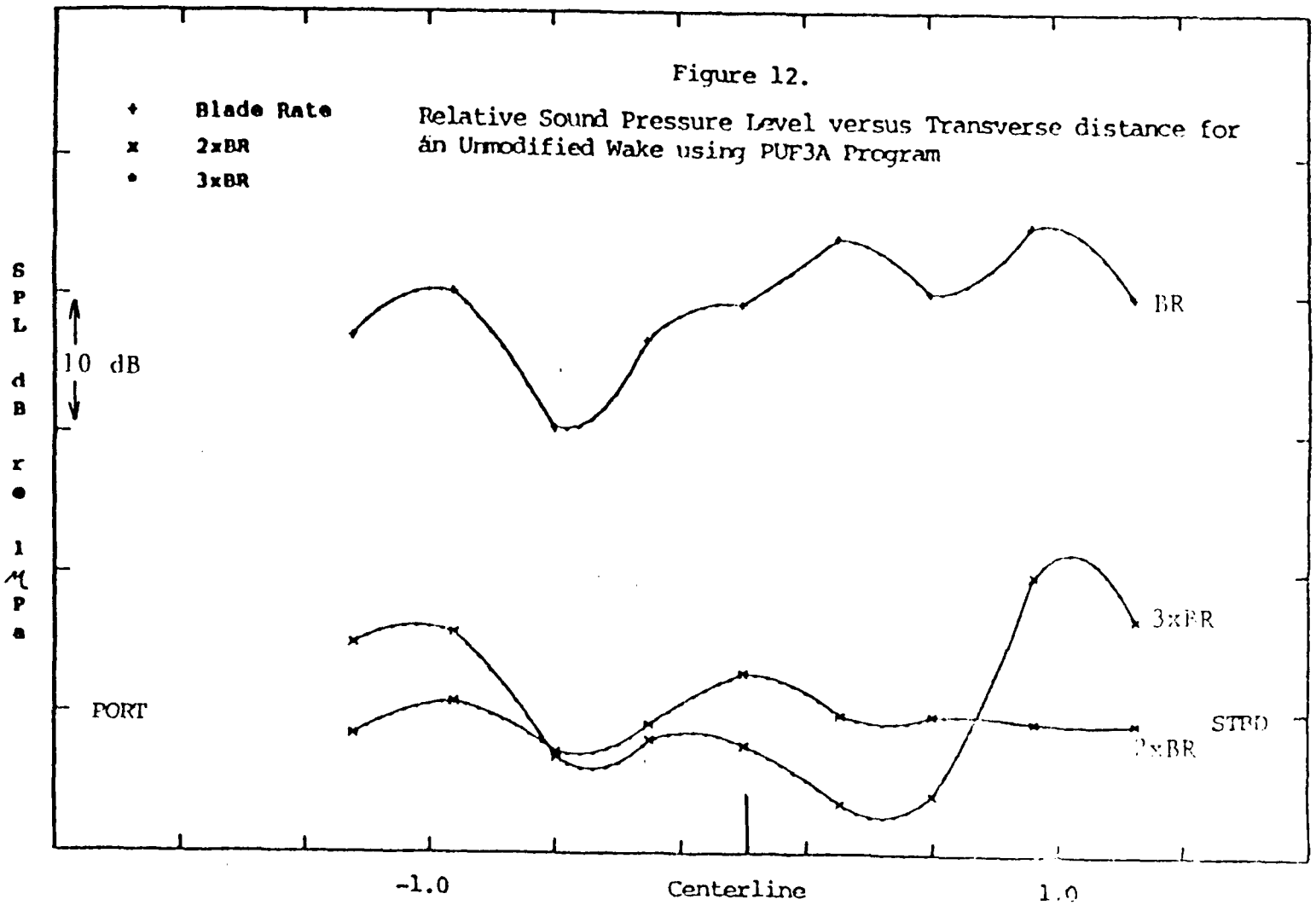

Relative Sound Pressure Level versus Transverse distance for an Unmodified Wake using PUF3A Program

Transverse Distance across Hullform Non-dimensionalized by Propeller Radius

Figure 13.

Relative Sound Pressure Level versus Transverse Distance for a Modified Wake in the Water Tunnel

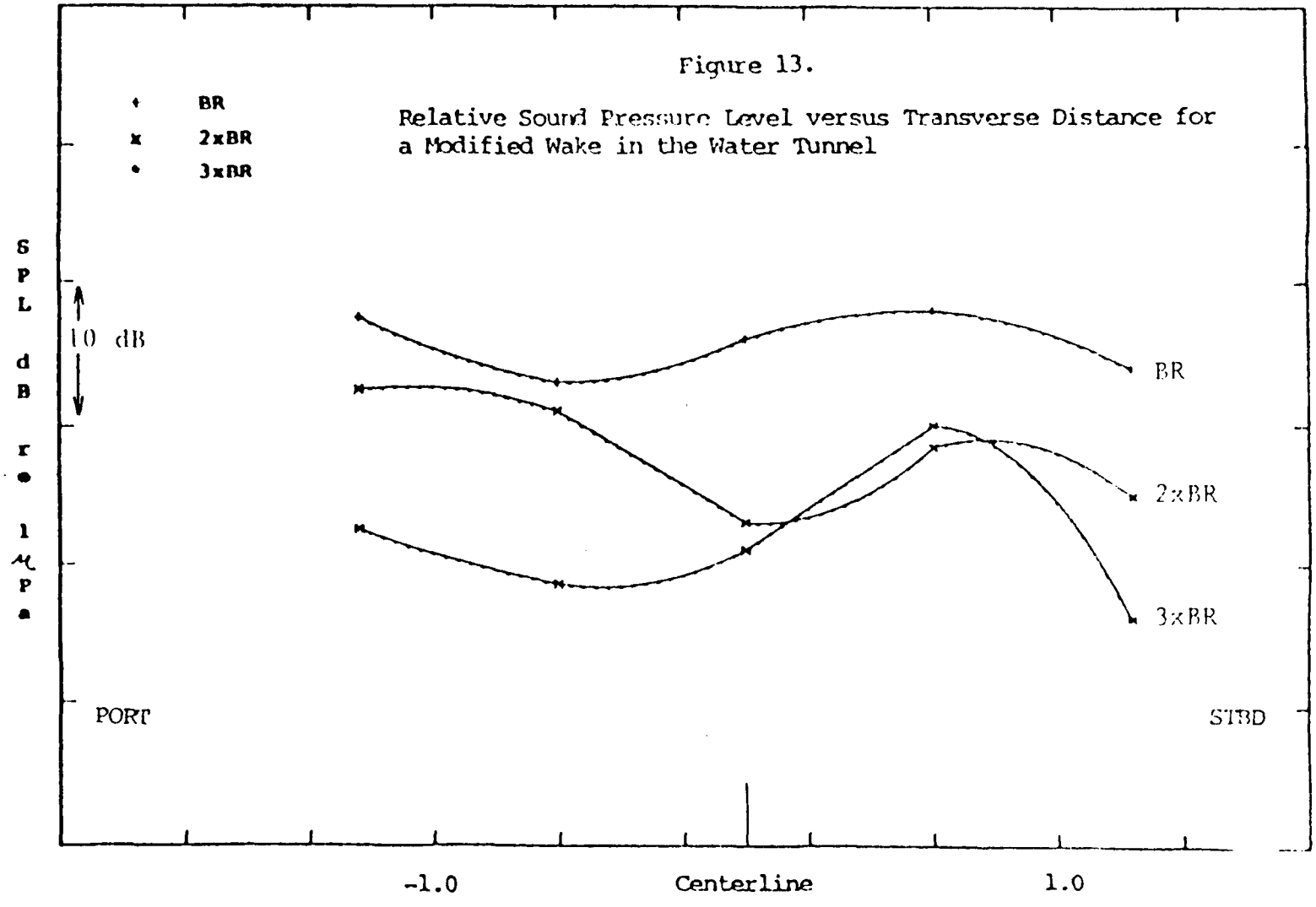

Transverse Distance across Hullform Non-dimensionalized by Propeller Radius

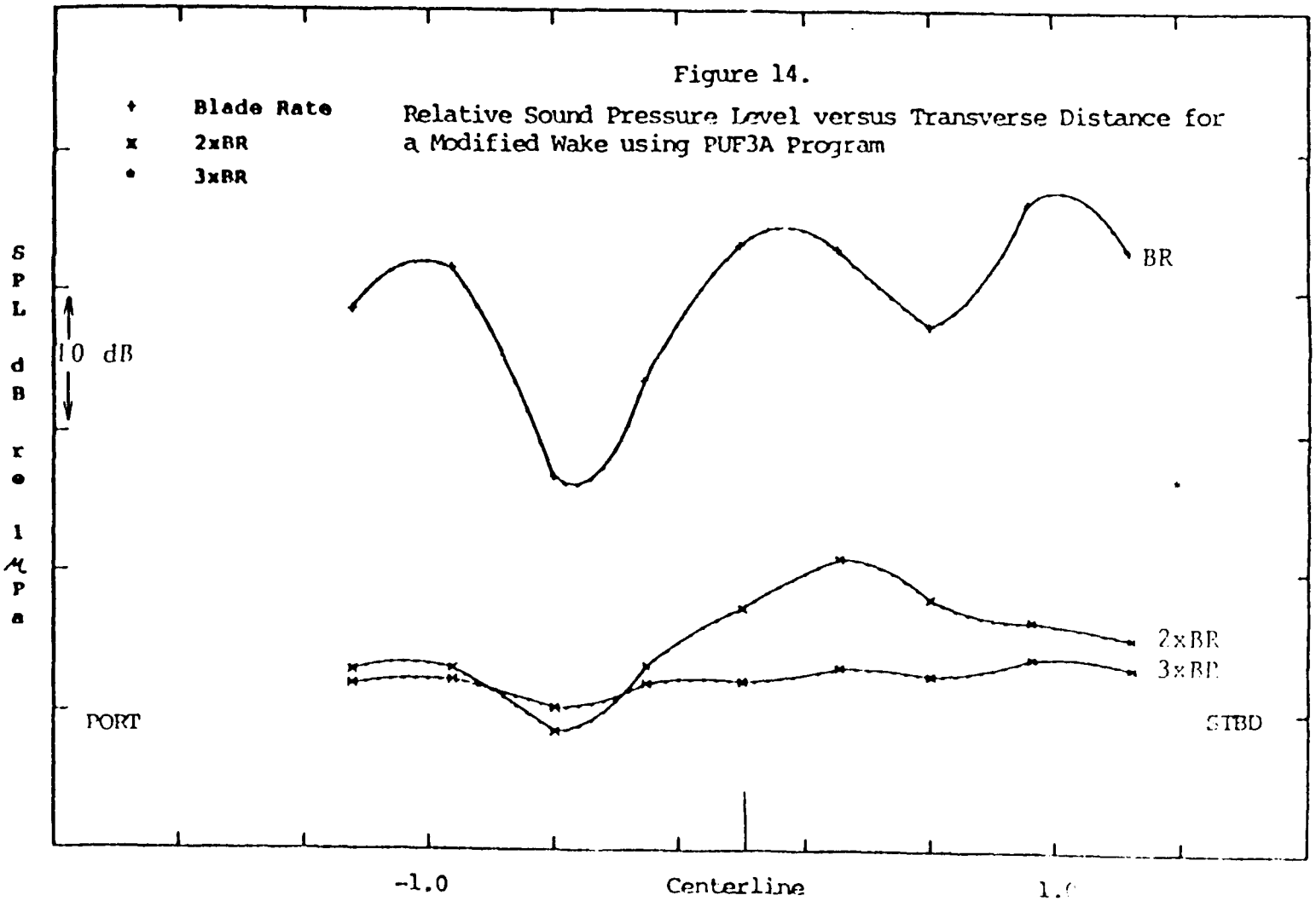

Figure 14.

Relative Sound Pressure Level versus Transverse Distance for a Modified Wake using PUF3A Program

Transverse Distance across Hullform Non-dimensionalized by Propeller Radius

Appendix A.

PROPELLER INPUT FILE

Table A-1. Propeller Input File

Propeller Geometry Input File for PUF3A 2/1990 edition

```
---- Propeller 1,  RH,  5 Blades ---
1       0       4       0      10       1
15      0       5
0.82    4.0     48.949
--- Non-dimensional Propeller Radius ---
0.2167 0.2500 0.3250 0.4000 0.4750 0.5500 0.6500 0.7000
1.1322 1.1243 1.1063 1.0883 1.0699 1.0508 1.0234 1.0082
0.0000 0.0000 0.0000 0.0000 0.0000 0.0000 0.0000 0.0000
0.0000 0.0000 0.0000 0.0000 0.0000 0.0000 0.0000 0.0000
0.2280 0.2469 0.2867 0.3237 0.3570 0.3861 0.4163 0.4252
0.0209 0.0228 0.0257 0.0268 0.0264 0.0247 0.0208 0.0186
0.0398 0.0372 0.0319 0.0272 0.0230 0.0192 0.0146 0.0126

0.7500 0.8000 0.8500 0.9000 0.9500 0.9800 1.0000
0.9916 0.9719 0.9489 0.9201 0.8871 0.8644 0.8476
0.0000 0.0000 0.0000 0.0000 0.0000 0.0000 0.0000
0.0000 0.0000 0.0000 0.0000 0.0000 0.0000 0.0000
0.4271 0.4217 0.4019 0.3611 0.2907 0.2061 0.0000
0.0162 0.0139 0.0116 0.0090 0.0060 0.0032 0.0000
0.0106 0.0089 0.0072 0.0058 0.0047 0.0043 0.0040
```

Appendix B.

MODEL WAKE PUF-3A INPUT FILE

Table B-1. Wake Input File for PUF-3A, Normal Wake

```
WATER TUNNEL WAKE INPUT FILE, PUF-3A, 2/1990 EDITION
WK= 5   NHARMA= 16   NHARMR= 16   NHARMT= 16   VOLWK= 1.000
----------WAKE RADII-----------------------------
0.3243  0.4865  0.6486  0.8108  1.0810
----------AXIAL VELOCITY COSINE HARMONICS--------
1.0100  0.9983  1.0420  0.9962  1.0230
-.0567  -.0314  -.0100  0.0014  0.0066
-.0551  -.0360  -.0164  -.0108  0.0090
-.0316  -.0248  -.0104  -.0064  0.0091
-.0095  -.0139  -.0032  -.0027  0.0042
0.0072  -.0047  -.0000  -.0000  0.0024
0.0178  0.0029  0.0040  0.0022  0.0015
0.0228  0.0077  0.0049  0.0022  0.0002
0.0211  0.0103  0.0054  0.0015  0.0013
0.0148  0.0108  0.0044  0.0008  0.0017
0.0088  0.0084  0.0030  -.0003  0.0031
0.0013  0.0064  0.0012  -.0018  0.0040
-.0055  0.0031  -.0010  -.0025  0.0045
-.0088  0.0006  -.0022  -.0032  0.0048
-.0094  -.0017  -.0036  -.0037  0.0049
-.0089  -.0031  -.0037  -.0035  0.0044
----------AXIAL VELOCITY SINE HARMONICS----------
0.0000  0.0000  0.0000  0.0000  0.0000
-.0087  -.0141  -.0172  -.0026  0.0001
0.0015  -.0036  -.0012  0.0019  0.0014
0.0006  -.0033  -.0007  0.0006  0.0009
0.0005  -.0038  -.0003  -.0002  0.0011
-.0012  -.0033  -.0014  -.0009  0.0002
0.0003  -.0015  -.0018  -.0005  0.0000
0.0000  -.0009  -.0013  0.0001  0.0003
0.0004  0.0008  -.0013  -.0005  0.0001
0.0006  0.0019  -.0011  0.0001  0.0002
0.0003  0.0017  -.0008  0.0001  0.0008
-.0004  0.0015  -.0004  0.0001  0.0005
-.0008  0.0014  -.0004  0.0002  0.0006
0.0006  0.0011  0.0008  0.0003  0.0005
0.0012  0.0004  0.0005  0.0006  0.0000
0.0012  0.0002  0.0004  0.0004  0.0001
```

Table B-1 (Continued)

----------RADIAL VELOCITY COSINE HARMONICS-------				
0.0182	0.0196	0.0310	0.0152	0.0247
-.6134	-.0871	-.1006	-.1042	0.1220
0.0059	0.0056	-.0025	-.0088	0.0175
0.0129	0.0095	0.0040	-.0010	0.0087
0.0147	0.0110	0.0083	0.0020	0.0034
0.0109	0.0103	0.0069	0.0027	0.0011
0.0059	0.0073	0.0060	0.0025	0.0006
0.0019	0.0062	0.0049	0.0021	0.0020
0.0005	0.0050	0.0043	0.0020	0.0027
-.0019	0.0033	0.0032	0.0016	0.0034
-.0028	0.0034	0.0023	0.0012	0.0026
-.0031	0.0024	0.0016	0.0008	0.0021
-.0025	0.0022	0.0010	0.0008	0.0019
-.0018	0.0017	0.0006	0.0008	0.0009
-.0016	0.0012	0.0007	0.0008	0.0004
-.0003	0.0006	0.0001	0.0004	0.0003
----------RADIAL VELOCITY SINE HARMONICS---------				
0.0000	0.0000	0.0000	0.0000	0.0000
-.0185	-.0113	-.0058	0.0045	0.0040
0.0005	0.0017	0.0010	0.0020	0.0024
0.0020	0.0010	0.0005	-.0001	0.0004
0.0014	0.0022	0.0011	0.0012	0.0014
0.0021	0.0020	0.0050	0.0008	0.0004
0.0030	0.0019	0.0005	-.0001	0.0003
0.0014	0.0021	0.0005	0.0004	0.0010
0.0014	0.0023	0.0002	0.0007	0.0008
0.0017	0.0012	-.0000	0.0004	0.0001
0.0006	0.0015	0.0004	0.0004	0.0001
0.0007	0.0009	0.0003	0.0001	0.0001
-.0003	-.0001	0.0003	0.0003	0.0008
0.0001	-.0002	0.0004	0.0002	0.0007
0.0002	0.0000	0.0005	0.0002	0.0007
-.0002	-.0004	0.0004	0.0002	0.0005

Table B-1. (Continued)

```
------TANGENTIAL VELOCITY COSINE HARMONICS-------
-.0153   -.0153   -.0003   -.0005   0.0071
0.0025   -.0065   -.0011   -.0037   0.0059
0.0014   0.0020   0.0019   0.0006   0.0017
0.0024   0.0049   0.0016   0.0009   0.0021
-.0039   0.0017   0.0012   -.0003   0.0007
-.0027   0.0018   0.0009   -.0002   0.0011
-.0011   0.0010   0.0006   0.0005   0.0003
0.0010   0.0005   0.0001   0.0008   0.0002
0.0001   -.0002   0.0001   0.0004   0.0005
0.0002   -.0003   -.0003   0.0004   0.0013
-.0001   -.0002   -.0002   0.0001   0.0002
0.0006   -.0001   -.0004   0.0002   0.0003
0.0003   -.0001   -.0000   -.0001   0.0003
0.0000   0.0001   0.0002   -.0001   0.0007
-.0000   -.0000   0.0004   -.0001   0.0007
-.0005   -.0001   0.0001   -.0001   0.0001
-------TANGENTIAL VELOCITY SINE HARMONICS--------
0.0000   0.0000   0.0000   0.0000   0.0000
-.2069   -.1782   -.1586   -.1450   0.1474
-.0114   -.0201   -.0200   -.0200   0.0228
0.0093   -.0059   -.0054   -.0089   0.0068
0.0115   -.0013   -.0010   -.0037   0.0024
0.0086   0.0017   0.0008   -.0012   0.0009
0.0081   0.0030   0.0013   -.0004   0.0026
0.0083   0.0035   0.0010   -.0002   0.0024
0.0059   0.0043   0.0010   -.0001   0.0020
0.0027   0.0035   0.0003   -.0001   0.0017
0.0013   0.0029   0.0001   -.0004   0.0007
-.0009   0.0023   -.0006   -.0006   0.0001
-.0016   0.0011   -.0008   -.0007   0.0003
-.0019   0.0005   -.0011   -.0009   0.0010
-.0023   -.0005   -.0009   -.0009   0.0011
-.0019   -.0008   -.0011   -.0007   0.0010
----------END OF WAKE INPUT FILE----------------
```

Appendix C.

MODEL MODIFIED WAKE PUF-3A INPUT FILE

Table C-1. Wake Input File for PUF-3A, Modified Wake

```
REACTION VANE WAKE - INPUT FILE FOR PUF3A 2/1990 EDITION
 NWK= 6  NHARMA= 16  NHARMR= 16  NHARMT= 16  VOLWK= 1.000
----------WAKE RADII----------
0.3243  0.4865  0.6486  0.8108  0.9189  1.0810
----------AXIAL VELOCITY COSINE HARMONICS----------
0.9774  0.9707  1.0310  0.9798  1.0230  1.0200
-.0096  -.0058  0.0193  0.0214  0.0244  0.0058
-.0373  -.0277  -.0111  -.0017  -.0044  0.0027
-.0320  -.0170  -.0111  -.0053  -.0099  0.0052
0.0024  0.0149  0.0106  0.0081  0.0049  0.0042
-.0041  0.0061  -.0009  -.0032  -.0008  0.0006
0.0150  0.0259  0.0158  0.0097  0.0094  0.0002
0.0154  0.0113  0.0089  0.0039  0.0023  0.0005
0.0100  0.0041  0.0108  0.0086  0.0041  0.0018
0.0202  0.0019  0.0075  0.0061  -.0037  0.0035
0.0000  -.0092  0.0026  0.0023  0.0033  0.0042
-.0419 -.03711  -.0253  -.0191  -.0064  0.0077
0.0314  -.0001  -.0077  -.0159  -.0132  0.0062
0.0214  0.0177  0.0128  0.0078  0.0033  0.0037
0.0099  0.0139  0.0018  -.0027  -.0082  0.0053
0.0026  0.0080  -.0005  -.0067  -.0071  0.0045
----------AXIAL VELOCITY SINE HARMONICS----------
0.0000  0.0000  0.0000  0.0000  0.0000  0.0000
-.0518  -.0432  -.0358  -.0158  -.0073  0.0054
-.0121  -.0202  -.0474  0.0023  0.0060  0.0003
-.0006  -.0148  -.0019  0.0053  0.0004  0.0004
0.0059  -.0128  -.0003  0.0034  0.0015  0.0007
0.0009  -.0057  -.0022  0.0010  0.0012  0.0001
0.0264  0.0220  0.0121  0.0062  0.0048  0.0010
0.0035  0.0096  -.0037  -.0075  -.0014  0.0011
0.0256  0.0293  0.0161  0.0060  0.0050  0.0016
0.0161  0.0107  0.0022  -.0027  -.0053  0.0012
0.0282  0.0180  0.0147  0.0070  -.0046  0.0020
-.0057  0.0014  0.0105  0.0122  0.0084  0.0004
-.0533  -.0516  -.0380  -.0288  -.0140  0.0034
0.0063  -.0084  -.0027  -.0030  0.0010  0.0008
0.0020  -.0084  -.0054  -.0008  0.0009  0.0003
-.0074  -.0052  -.0055  -.0017  -.0031  0.0003
```

Table C-1. (Continued)

----------RADIAL VELOCITY COSINE HARMONICS---------					
-.0526	-.0245	-.0544	-.0254	-.0500	0.0117
-.0557	-.0574	-.0561	-.0594	-.0619	0.0883
-.0201	-.0082	-.0040	-.0061	-.0050	0.0083
0.0042	0.0185	0.0168	0.0123	0.0062	0.0040
0.0117	0.0122	0.0066	0.0030	0.0023	0.0001
0.0162	0.0177	0.0161	0.0131	0.1381	0.0086
0.0279	0.0178	0.0028	-.0059	-.0031	0.0005
0.0075	0.0060	0.0081	0.0104	0.0138	0.0056
0.0206	0.0159	0.0028	-.0063	-.0068	0.0011
0.0063	0.0037	0.0036	0.0000	-.0044	0.0010
0.0043	0.0024	0.0004	-.0129	-.0198	0.0055
-.0103	-.0074	-.0057	-.0193	-.0391	0.0074
-.0213	-.0225	0.0048	0.0277	0.0358	0.0066
0.0030	0.0007	-.0012	-.0004	0.0061	0.0011
0.0059	0.0009	-.0002	0.0010	-.0049	0.0005
-.0005	-.0027	-.0031	0.0016	-.0008	0.0017
----------RADIAL VELOCITY SINE HARMONICS----------					
0.0000	0.0000	0.0000	0.0000	0.0000	0.0000
0.0147	0.0234	0.0156	0.0205	0.0034	0.0097
0.0042	0.0075	0.0089	0.0093	0.0085	0.0052
0.0155	0.0099	0.0043	0.0021	-.0009	0.0007
-.0232	-.0106	0.0052	0.0105	0.0097	0.0055
0.0039	0.0056	0.0036	0.0009	0.0002	0.0008
-.0027	0.0009	0.0104	0.0150	0.0137	0.0067
-.0093	-.0043	-.0010	0.0012	0.0040	0.0046
0.0139	0.0086	0.0085	0.0150	0.0203	0.0073
-.0031	-.0009	-.0008	0.0057	0.0080	0.0050
0.0088	0.0104	0.0080	0.0104	0.0185	0.0044
0.0162	0.0145	-.0017	-.0211	-.0293	0.0061
-.0238	-.0098	-.0024	-.0134	-.0302	0.0048
-.0068	-.0064	0.0039	0.0113	0.0188	0.0011
-.0080	-.0052	-.0001	-.0028	-.0017	0.0017
-.0056	-.0008	0.0008	-.0016	-.0082	0.0018

Table C-1. (Continued)

```
----------TANGENTIAL VELOCITY COSINE HARMONICS-----
0.1802   0.1832   0.1579   0.0961   0.0556   0.0189
0.0046   0.0032   0.0023   0.0021   0.0160   0.0054
-.0080   -.0020   -.0060   -.0079   -.0103   0.0037
-.0171   0.0010   0.0027   -.0003   -.0078   0.0008
-.0083   -.0105   -.0122   -.0070   0.0035   0.0022
-.0096   0.0006   0.0032   0.0029   0.0019   0.0006
-.0121   -.0073   -.0124   -.0085   0.0027   0.0042
-.0032   -.0009   0.0003   0.0014   0.0030   0.0015
-.0016   -.0008   -.0015   -.0036   -.0119   0.0017
-.0081   -.0066   -.0043   -.0083   -.0015   0.0037
-.0016   -.0028   0.0022   0.0055   0.0054   0.0046
0.0197   0.0103   0.0131   0.0167   0.0104   0.0030
0.0029   0.0028   0.0000   -.0019   -.0031   0.0022
0.0004   0.0031   0.0017   0.0027   -.0081   0.0007
0.0011   0.0006   0.0014   0.0028   0.0030   0.0004
-.0016   -.0003   -.0007   0.0015   0.0055   0.0011
----------TANGENTIAL VELOCITY SINE HARMONICS-------
0.0000   0.0000   0.0000   0.0000   0.0000   0.0000
-.0782   -.0278   -.0309   -.0657   -.1109   0.1612
-.0123   -.0025   -.0029   -.0081   -.0054   0.0219
0.0115   0.0059   0.0017   -.0020   -.0113   0.0098
0.0227   0.0085   0.0067   0.0050   0.0012   0.0001
0.0106   0.0050   0.0053   0.0070   0.0048   0.0018
0.0140   0.0080   0.0032   0.0050   0.0091   0.0048
0.0062   0.0063   0.0074   0.0082   0.0058   0.0011
0.0036   0.0038   0.0002   0.0014   0.0111   0.0052
0.0033   0.0035   0.0016   0.0003   -.0018   0.0033
0.0008   0.0004   -.0020   -.0073   -.0142   0.0048
-.0148   -.0080   -.0109   -.0184   -.0090   0.0059
0.0010   -.0035   0.0026   0.0026   -.0020   0.0054
0.0089   0.0027   0.0034   0.0020   0.0075   0.0006
0.0035   0.0024   0.0009   -.0021   -.0062   0.0012
0.0004   0.0013   0.0005   -.0012   -.0087   0.0011
----------END OF WAKE INPUT FILE-------------------
```

Appendix D.

FIELD POINT POTENTIAL OUTPUT FILE

Table D-1. Field Point Locations Input File, for PUF3FPP, on the Model Afterbody

(inches)		
Axial	Radial	Angular
0.0000	1.5178	3.1416
0.0000	2.1575	2.5255
0.0000	1.7086	2.7838
0.0000	1.7086	3.4994
0.0000	2.1575	3.7577
0.0000	1.8713	2.6250
0.0000	1.5655	2.9461
0.0000	1.5655	3.3371
0.0000	1.8713	3.6582

* Reference Point is the center axis of the propeller shaft and the axial center of the hub.

Appendix E.

HYDRODYNAMIC PARAMETERS FOR PUF-3A INPUT

Table E-1. Hydrodynamic Parameters for PUF-3A Input

Advance Ratio - $J_S = V_S/nD$

Froude Number - $Fn = n^2 D/g_c$

Cavitation Index - $\sigma_s = \frac{(P - P_v)\, g_c}{.5\, \rho\, n^2\, D^2}$

Table E-2. Water Tunnel Test Data

		Normal Wake		Modified Wake
Ship's Speed	V_S	28.2	ft/sec	27.1
Propeller RPM	$60 \cdot n$	2717.	RPM	2562.
Propeller Dia.	D	9.2237	inches	9.2237
Press at Prop	P	22.6	PSIA	25.5
Advance Ratio	J_S	0.81		0.83
Froude No.	Fn	48.95		43.52
Cavitation Index	σ_s	4.0		5.0
Gravitational Const	g_c	32.2	lbm/lbf ft/sec^2	
Vapor Pressure	P_v	0.33	PSIA	
Density of Water	ρ	62.4	lbs/ft^3	